A MEASUREMENT OF THE LINEWIDTH OF A LASER OSCILLATOR

by

John Arthur Hanlon

A Dissertation Submitted to the Faculty of the

DEPARTMENT OF ELECTRICAL ENGINEERING

In Partial Fulfillment of the Requirements
For the Degree of

DOCTOR OF PHILOSOPHY

In the Graduate College

THE UNIVERSITY OF ARIZONA

1 9 7 1

THE UNIVERSITY OF ARIZONA

GRADUATE COLLEGE

I hereby recommend that this dissertation prepared under my direction by John Arthur Hanlon

entitled A MEASUREMENT OF THE LINEWIDTH OF A LASER OSCILLATOR

be accepted as fulfilling the dissertation requirement of the degree of Doctor of Philosophy

S. F. Jacobs — 8-3-71

Dissertation Director — Date

After inspection of the final copy of the dissertation, the following members of the Final Examination Committee concur in its approval and recommend its acceptance:*

Roy H. Mattson	8-9-71
Roger C. Jones	8/9/71
Marlan O. Scully	8/9/71
[illegible]	8/11/71
Donald R. Hoffman	8/11/71

*This approval and acceptance is contingent on the candidate's adequate performance and defense of this dissertation at the final oral examination. The inclusion of this sheet bound into the library copy of the dissertation is evidence of satisfactory performance at the final examination.

STATEMENT BY AUTHOR

This dissertation has been submitted in partial fulfillment of requirements for an advanced degree at The University of Arizona and is deposited in the University Library to be made available to borrowers under rules of the Library.

Brief quotations from this dissertation are allowable without special permission, provided that accurate acknowledgment of source is made. Requests for permission for extended quotation from or reproduction of this manuscript in whole or in part may be granted by the head of the major department or the Dean of the Graduate College when in his judgment the proposed use of the material is in the interests of scholarship. In all other instances, however, permission must be obtained from the author.

SIGNED: John Arthur Hanlon

ACKNOWLEDGMENTS

The completion of this study would not have been possible without the encouragement and patience of many people. In particular I want to thank my wife, Colleen, and family, Michael, Carrie, Jeanne, Catherine, and John Patrick for their patience, encouragement, and persistence; my parents for encouragement and financial help; my advisor, Steve Jacobs, for his patience; Dick Sumner, who made the many pieces of optics that I needed; John Poulos for his excellent help in thin films and vacuum techniques, encouragement, and friendship; the Electrical Engineering and Optical Science Departments for their financial aid and academic opportunities; and the many friends around the University and in Tucson for their interest in my well-being and encouragement to finish my work.

TABLE OF CONTENTS

TABLE OF CONTENTS--Continued

LIST OF ILLUSTRATIONS

LIST OF ILLUSTRATIONS--Continued

LIST OF TABLES

ABSTRACT

Measurements of the inherent oscillation linewidth of a single-mode, 3.39μ He-Ne laser are described. The output beams of two independent lasers, superimposed and focused onto the surface of a photodiode, resulted in a beat frequency which was displayed on a panoramic spectrum analyzer. This technique was used previously by several investigators to study gas laser linewidth; however, the linewidth due to quantum noise was nearly always masked by effects of environmental perturbations.

In this study two lasers are built into a single block of quartz, so that they share very similar environments, and only differential perturbations affect the beat note. A low Q resonator was used so that the laser oscillation linewidth was quite broad, and could be made to exceed the masking effects of environmental broadening and measured. The oscillation linewidth of the local oscillator was much narrower than that of the test laser, so that the spectral density of the observed beat approximates the spectral density of the test oscillator convolved with the spectrum analyzer resolution.

Oscillation linewidths due to quantum noise were observed; a linewidth as broad as 5.5 KHz near oscillation threshold was measured. Also measured was the stability of

the single block, dual-laser design concept. During times less than 100 milliseconds the average length of two lasers in a single quartz block changed by the same amount to the order of 10^{-11} cm--approximately 1/200 the size of an atom.

In addition, a simple theoretical analysis based on a model related to laser processes was used to derive an expression for the oscillation linewidth. Previous treatments either used artificial assumptions or required a detailed quantum mechanical argument to derive the oscillation linewidth formula. Also presented is a more detailed analysis using Feynman path integral techniques that includes the effects on the oscillation linewidth of amplitude noise, atomic-line broadening, and saturation.

CHAPTER I

INTRODUCTION

In recent years the usefulness of lasers has been well established. The optical properties of laser light, particularly the high degree of monochromaticity and high intensity, have made it a suitable source for a large variety of uses. Many useful laser systems have been built that have analogs at lower frequencies. Communication systems, radars, and pulse generators are examples. As at lower frequencies, stable oscillators are a basic component in many systems, and much research has been directed toward making stable laser oscillators and studying the noise properties of laser light. In this dissertation laser light phase fluctuations caused by quantum noise will be studied.

The causes for noise in laser light can be several. First, and ordinarily the most important, are man-made disturbances such as acoustical and mechanical noise that change the physical length of the resonant cavity in an unpredictable way. Their effect is to change the relative position of the cavity and atomic resonances, since a cavity length change ΔL causes the cavity resonant frequency, ν, to change an amount $\Delta\nu = \frac{\Delta L}{L}\nu$.

The consequence is that the round trip gain, and the frequency for which the round trip phase shift is a multiple of 2π, fluctuate in an unpredictable way giving rise to amplitude and frequency flutter in the output laser light. If these sources of noise are reduced, a second noise source, quantum noise, predominates and ultimately limits the purity of the output laser light.

Quantum noise is caused by spontaneous emission of photons into the cavity mode, either from atoms inside the cavity, or by the ordinarily negligible contribution due to photons that enter the cavity mode through the mirrors and come from outside the laser cavity. The fact that the starting phase of the standing wave caused by these monochromatic photons is completely random, and only describable in a probabilistic way, is the primary cause of laser light noise due to quantum effects. Measures of this noise are the photon statistics and the spectral densities of the amplitude and phase fluctuations. Armstrong and Smith (1965), Arecchi, Degiorgio, and Querzola (1967), and others have made careful measurements of amplitude fluctuations caused by quantum noise for laser oscillators operating below, at, and above oscillation threshold. Phase fluctuations caused by quantum noise have been less thoroughly studied, because in most lasers phase fluctuations caused by man-made disturbances are predominant and mask their effects. However, quantum noise phase

fluctuations are important in special applications. For example, in optical frequency standards, the best possible laser stability is required, so that man-made noises must be reduced to a minimum. Such lasers are ideally limited in stability only by phase fluctuations caused by quantum noise.

Phase fluctuations are measured by mixing the light from independent lasers and by observing the spectrum of the beat note. For identically designed laser oscillators the beat note at the difference frequency has fluctuations that are larger than the fluctuations in either laser. A radio-frequency spectrum analyzer directly measures the spectral profile of the beat note. Since the spectral profile measured in this way is normally due to man-made noise, special techniques have been developed to measure the narrow quantum noise spectral profile. One such technique, developed by Siegman, Diano, and Manes (1967), is to measure the power spectrum of the beat note after it has passed through a frequency discriminator. This technique has been successfully applied to He-Ne lasers, and it is successful because the effects of the masking noise and quantum noise can be separated. As shown by Siegman et al. (1967) man-made disturbances have a $1/f^2$-type spectrum at the discriminator output, while quantum noise contributes a flat noise spectrum proportional to the laser oscillation linewidth. Figure 1 is a plot of the spectral density of

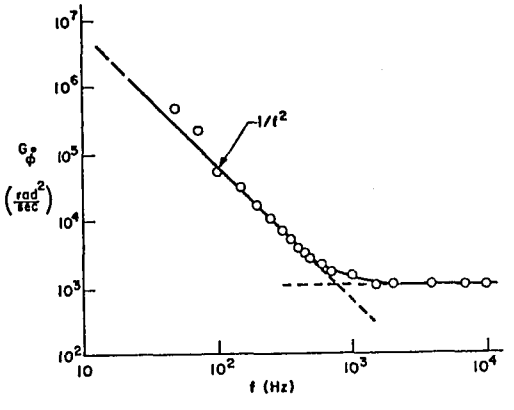

Fig. 1. An Indirect Measurement of the Oscillation Linewidth of a 6328μ He-Ne Gas Laser

the instantaneous fluctuations in the 30 MHz beat note between two He-Ne 6328μ gas lasers, measured by scanning the video output of 30 MHz discriminator with an audio wave analyzer.

Even though these indirect measurements of the oscillation linewidth have been successful, the alternate technique to measure the quantum noise profile directly is still of interest. Recently a direct measurement of the spectral profile of a $Pb_{088}\ Sn_{012}\ Te$ diode laser was accomplished by Hinkley and Freed (1969). A picture of the r-f spectrum due to quantum noise for a diode laser is shown in Fig. 2. Diode lasers have large oscillation linewidths that are not so easily masked by man-made noise sources, even when operating well above threshold.

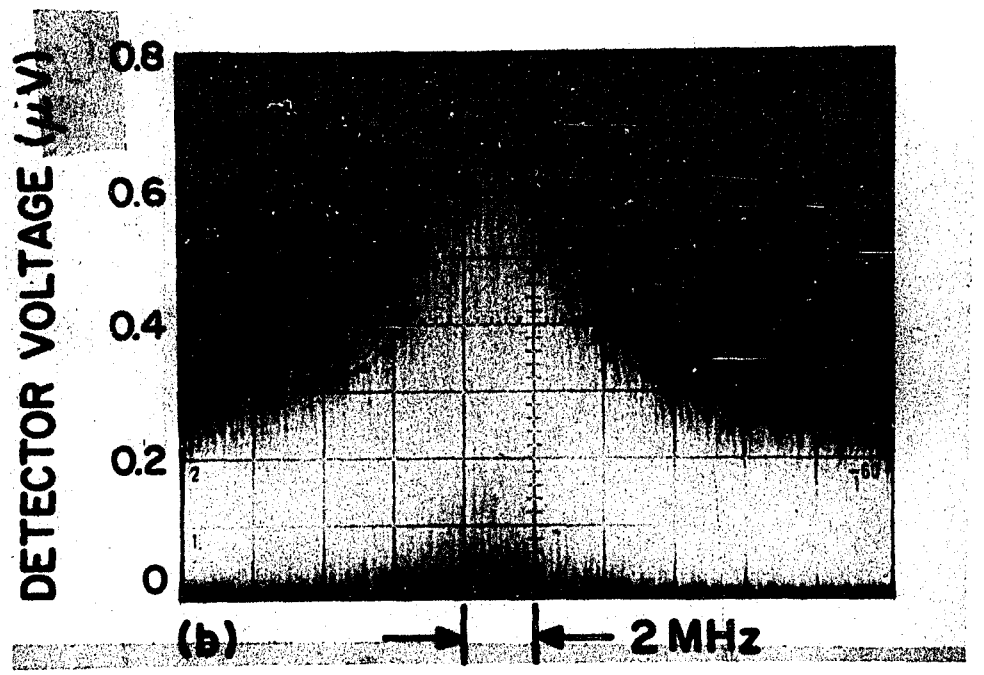

Fig. 2. A Direct Oscillation Linewidth Measurement of a PbSnTe Diode Laser

This dissertation is concerned with the phase fluctuations of a 3.39μ He-Ne gas laser. The primary objective of the study is the following:

To measure directly the frequency spectrum of the beat note between two independently operated 3.39μ He-Ne lasers built into a single quartz block, and to determine how closely it is due to quantum phase noise. This problem has been chosen because direct observations of the spectral profile of a gas laser due to quantum noise have not been made.

A subsidiary problem is to give a consistent, intuitive description of phase noise in a laser oscillator. Previous treatments either use somewhat artificial assumptions to obtain an expression for the linewidth, or the argument is difficult to understand because it is an end result of a detailed quantum mechanical calculation. What is needed is a consistent, descriptive treatment that may be used in a first course on lasers, where there is not time for a detailed quantum mechanical argument to explain the important idea of oscillation linewidth. My idea of such a treatment is presented in Chapter II. Chapter III contains a discussion of the general design philosophy, the laser design, and the equipment used to measure the spectral profile of a 3.39μ He-Ne laser. Chapter IV is a discussion of the linewidth measurements taken during this study, and a summary of the results of the dissertation research.

CHAPTER II

THEORY

The Noise Properties of Laser Oscillators

The output of a stable, single frequency laser oscillator is a nearly ideal optical sine wave, with nearly constant amplitude and frequency. However, even the output from the most stable laser fluctuates in amplitude and phase due to various man-made disturbances and to photons spontaneously emitted into the resonant cavity.

In this chapter we will analyze the source and effects of quantum noise on the output of a laser oscillator. It will be shown how quantum noise causes the standing wave field inside the laser resonator, and therefore also the output laser light, to fluctuate in amplitude and phase. These fluctuations cause the oscillation amplitude and frequency to be uncertain and only a statistical measure of them can be given. When quantum noise is the predominant effect, a commonly used measure of the phase fluctuations is the width of the spectral profile (oscillation linewidth) of the standing wave field centered about the oscillation frequency. An expression for the oscillation linewidth will be derived.

An interesting technique to study noise properties is by Feynman path integral techniques. This technique is summarized, and then used to describe in more detail laser oscillator noise, including the effects on the oscillation frequency of amplitude noise, atomic line broadening, and saturation.

A Model for Laser Photons

In this section a consistent physical model is used to show how spontaneous emission causes amplitude and phase fluctuations in the standing wave field of a laser oscillator. Strictly speaking, amplitude and phase fluctuations in an oscillator should not be considered independently because an oscillator must of necessity be a nonlinear device; the nonlinearity couples amplitude and phase. However, for lasers operating enough above threshold so that the fluctuating field is small compared to the steady state field, the driving force separates into amplitude and phase dependent terms. In this case it is a good approximation to consider amplitude and phase fluctuations independently.

An often misused concept is that the photons in the laser resonator bounce back and forth between the mirrors and are localized like billiard balls. But localization of a photon requires that it be described by a wave packet, and to construct a wave packet requires the superposition

of many frequencies. However, a laser above threshold is essentially a single frequency device and a photon inside the resonator is better described by a standing wave. Figure 3 illustrates the idea. In this picture, each time a photon is added to the cavity, an excitation, that is a small amplitude standing wave, is added to the cavity. Thus the "photon" is present everywhere simultaneously.

As is well known, photons can be added to the laser cavity by either *stimulated* or *spontaneous emission*. This model gives a physical picture of the difference between these mechanisms. Monochromatic photons, born by stimulated emission, add a standing wave field in phase with the stimulating standing wave field, whereas the starting phase of each spontaneously emitted photon, although definite, can have any value between zero and 2π. Since there is no preference for a particular starting phase, all starting phases must be considered equally likely. Thus, if θ_i represents the starting phase of the standing wave field of a single photon, then the probability, $p(\theta_i)$ that θ_i is in the range $d\theta_i$ is given by

$$p(\theta_i)d\theta_i = \frac{1}{2\pi} d\theta_i$$

Using this model the width of the laser oscillation linewidth can be derived and then shown to be in agreement with that derived using the complete quantum laser theory of Scully and Lamb (1966).

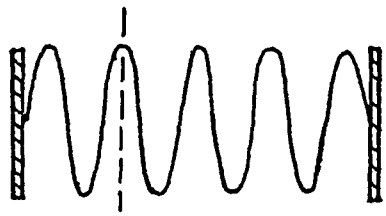

The standing wave field $E_o \cos \omega_o t \sin kz$.

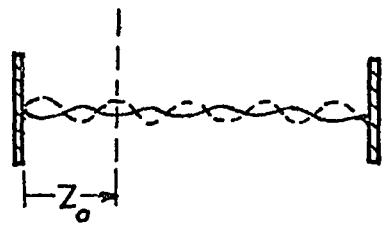

The standing wave field of two spontaneously emitted photons. $E_i = \Delta E \cos(\omega_o t + \theta_i) \sin kz$. The photons shown had different starting phase.

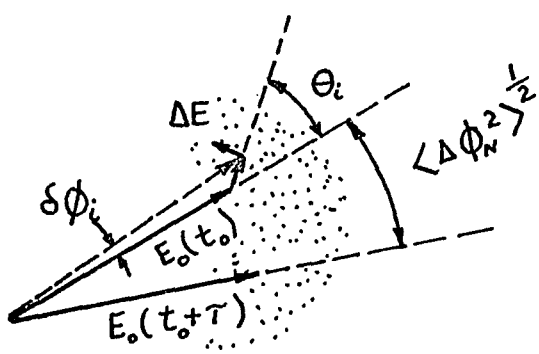

A phasor diagram of the field amplitude at the position of a standing wave peak during the time $t_o < t < t_o + \tau$.

Fig. 3. The Effects of Spontaneous Emission

The Spectral Density of the Standing Wave Field Amplitude

In order to mathematically describe the random properties of the electric field it is necessary to use the theory of random processes. In this theory the Fourier transform relationship between the correlation function and the spectral density is a fundamental concept. In the following paragraphs it will be used to find the spectral density of laser oscillator frequency fluctuations.

An expression for the standing wave field amplitude inside a resonator can be written as

$$E(t) = |E(t)|\cos\left(\omega_o t + \phi(t)\right)$$

Here ω_o is the optical frequency of the oscillating mode, and the functions $|E(t)|$ and $\phi(t)$ are slowly varying real random functions of time.

Let the analytic signal associated with $E(t)$ be

$$\tilde{E}(t) = |E(t)|e^{i\omega_o t + \phi(t)}$$

Then the complex correlation function,

$$\underset{\tilde{E}}{R}(\tau) = \langle \tilde{E}(t)\ \tilde{E}(t+\tau)^* \rangle$$

$$= \langle |E(t)||E(t+\tau)|e^{-i\omega_o \tau}\ e^{i\left|\phi(t)-\phi(t+\tau)\right|} \rangle$$

If it is assumed that the probability distributions for amplitude and phase fluctuations are independent, the

correlation function of the field, $\tilde{R}_{\tilde{E}}(\tau)$, can be factored into a product. So that,

$$\tilde{R}_{\tilde{E}}(\tau) = \langle |E(t)||E(t+\tau)| \rangle \langle e^{+i\left[\phi(t)-\phi(t+\tau)\right]} \rangle e^{-i\omega_o \tau}$$

The one sided spectral density of the total field, $S_E(\omega)$, is defined by

$$S_E(\omega) = \frac{1}{4}\int_{-\infty}^{\infty} \tilde{R}_{\tilde{E}}(\tau) e^{+i\omega\tau} d\tau = \frac{1}{4}\left[S_{|E|}^{(\omega-\omega_o)} * s_{\phi}(\omega-\omega_o) \right.$$

where * denotes a convolution operation, and

$$S_{|E|}^{(\omega-\omega_o)} \equiv \int_{-\infty}^{\infty} \langle |E(t)||E(t+\tau)| \rangle e^{+i(\omega-\omega_o)\tau} d\tau$$

and

$$s_{\phi}(\omega-\omega_o) \equiv \int_{-\infty}^{\infty} \langle e^{+i\left[\phi(t)-\phi(t+\tau)\right]} \rangle e^{+i(\omega-\omega_o)\tau} d\tau$$

In Appendix A it is shown that the amplitude spectrum, $S_{|E|}^{(\omega-\omega_o)}$, is small and broad, so that phase noise makes the predominant contribution to the total spectrum. It is also shown in the appendix that in a heterodyne experiment as described in Chapter III the spectral density of the detected signal is $S_E(\omega_2-\omega_1)$. Because the contribution of the amplitude spectral density is small, the shape of the measured spectrum approximates $s_{\phi}(\omega_2-\omega_1)$. Here ω_1 and ω_2 are two independent laser frequencies.

Neglecting amplitude fluctuations, phase fluctuations are considered for a constant amplitude standing wave field

$$\mathbf{E}(t) = E_o \cos\left(\omega_o t + \phi(t)\right)$$

Here $\phi(t)$ is a stationary random process. The spectral density of this field is given by

$$S_{\mathbf{E}}(\omega) \equiv S_{\phi}(\omega) = \frac{E_o^2}{4} s_{\phi}(\omega-\omega_o)$$

$$= \frac{E_o^2}{4} \int_{-\infty}^{\infty} \langle e^{i\left|\phi(0)-\phi(\tau)\right|} \rangle \; e^{+i(\omega-\omega_o)\tau} d\tau$$

It is shown in the following section that the probability distribution of the phase accumulation in a time τ, $\phi(\tau) - \phi(0)$, is Gaussian, so that

$$\langle e^{i\left|\phi(0)-\phi(\tau)\right|} \rangle = e^{-1/2\langle\left|\phi(\tau)-\phi(0)\right|^2\rangle}$$

and therefore,

$$S_{\phi}(\omega) = \frac{E_o^2}{4} \int_{-\infty}^{\infty} e^{-1/2\langle\left|\phi(\tau)-\phi(0)\right|^2\rangle} \; e^{+i(\omega-\omega_o)\tau} d\tau \qquad (1)$$

Refer to the model for a laser photon and in particular to Fig. 3. The random part of the phase develops as a series of random steps of approximate length

$$\delta\phi_i \simeq \frac{\Delta E}{E_o} \sin\theta_i \qquad (2)$$

The phase angle makes a one-dimensional random walk with variable step size. Reif (1965) discusses this problem in detail. For such problems, the mean squared displacement in a time τ is equal to the number of steps in time τ multiplied by the mean squared step size. Thus,

$$\begin{aligned} \langle \Delta\phi_\tau^2 \rangle &= \langle \left| \phi(\tau) - \phi(0) \right|^2 \rangle \\ &= N \langle (\delta\phi_i)^2 \rangle \\ &\equiv D|\tau| \end{aligned} \tag{3}$$

Here N denotes the average number of steps in time τ, and $\langle (\delta\phi_i)^2 \rangle$ denotes the mean squared step size. The constant D is often referred to as the diffusion constant. Using Eq. (3) in Eq. (1) the spectral density becomes

$$\begin{aligned} S_\phi(\omega) &= \frac{E_o^2}{4} \int_{-\infty}^{\infty} e^{-1/2D|\tau|} \, e^{-i(\omega-\omega_o)\tau} \, d\tau \\ &= \frac{E_o^2}{4} \frac{D}{(\omega-\omega_o)^2 + (D/2)^2} \end{aligned} \tag{4}$$

The full width at half maximum of this Lorentzian spectral density is defined to be the laser oscillation linewidth, $\Delta\omega_o$. It is equal to the constant D.

The usual expression for the linewidth can be found by relating D to laser parameters. To do this, it is necessary to calculate the number of steps in time τ and the mean squared step size for use in Eq. (3).

The mean squared step size can be calculated in the following way. Each photon, added to a single mode of the cavity, increases the energy by an amount (in mks units)

$$\hbar\omega_o = \frac{\epsilon_o (\Delta E)^2 V}{4} \tag{5}$$

where ΔE is the maximum value of the added standing wave electric field, V is the volume of the cavity mode, and ω_o is the circular frequency of the oscillation. The standing wave, added to the cavity by a photon therefore, has a peak amplitude

$$E_i = \Delta E \cos(\omega_o t + \theta_i)$$

$$= \left(\frac{\hbar\omega_o}{\epsilon_o V}\right)^{1/2} 2 \cos(\omega_o t + \theta_i)$$

Here θ_i is the phase of the added field. The electric field, caused by photons added to the cavity as a result of stimulated emission, is in phase with the large stimulating field E_o. Therefore, for these photons $\theta_i = 0$; they do not perturb the phase. The field, caused by spontaneously emitted photons, has no phase relationship either to the field E, or to other spontaneously emitted photons; they are equally likely to have any starting phase between 0 and 2π. For these photons the probability distribution for θ_i is uniform. Thus

$$p(\theta_i)d\theta_i = \frac{1}{2\pi} d\theta_i$$

Using this probability distribution the mean squared step size can be easily calculated. Using Eq. (2) and Eq. (5),

$$\langle(\delta\phi_i)^2\rangle = \left(\frac{\Delta E}{E_o}\right)^2 \int_0^{2\pi} \sin^2\theta_i \frac{d\theta_i}{2\pi}$$

$$= \left(\frac{\Delta E}{E_o}\right)^2 \frac{1}{2}$$

$$= \frac{2\hbar\omega}{\epsilon_o V E_o^2} \qquad (6)$$

Next, the average number of steps taken in a time τ will be calculated. The number of phase steps is equal to the average number of random phase events that occur during the time interval τ. As stated in the introduction, random phase photons have two sources:

1. Photons from the external environment that enter the cavity mode through the mirrors.
2. Spontaneously emitted photons from atoms inside the laser cavity.

Consider first the rate at which photons are added to the passive cavity mode because of its contact with the external environment.

Any cavity in thermal equilibrium at temperature T has $\bar{n}+1/2$ photons per mode. The average number of photons, $\bar{n}$, is given by the Planck distribution, where

$$\bar{n} = \frac{1}{e^{\frac{h\omega_o}{kT}} - 1} \tag{7}$$

Each photon in the mode has an average lifetime, t_p, related to the cavity full width, $\Delta\omega_c$, the quality factor Q, and the resonant frequency, ω_o, in the usual way by the following equation:

$$t_p = \frac{Q}{\omega_o} = \frac{1}{\Delta\omega_o}$$

In equilibrium the average number of photons lost from the cavity mode in a time τ is written as

$$N = \frac{p\tau}{h\omega_o} = \frac{\omega_o \langle W \rangle}{Q} \frac{\tau}{\hbar\omega_o} = (\bar{n}+1/2)\tau/t_p \tag{8}$$

Here p is the power output of the passive cavity mode due to all mechanisms, and $\langle W \rangle$ is the average energy stored in the passive cavity mode.

Since the cavity is in equilibrium, $(\bar{n}+1/2)\tau/t_p$ must also equal the number of phase steps, or the number of random phase photons entering the passive cavity end mirrors during the same time.

In summary:

$$\langle (\Delta\phi_\tau)^2 \rangle = D|\tau| = N\langle (\delta\phi_i)^2 \rangle \tag{3}$$

$$\langle (\delta\phi_i)^2 \rangle = \frac{2\hbar\omega_o}{\epsilon_o V E_o^2} \tag{6}$$

$$N = (\bar{n}+1/2)\frac{\tau}{t_p} \tag{8}$$

$$\bar{n} = \frac{1}{e^{\frac{\hbar\omega_o}{kT}} - 1} \tag{7}$$

Therefore, the passive cavity contribution to $\Delta\omega_o$ is

$$\frac{N\langle(\delta\phi_i)^2\rangle}{|\tau|} = \frac{2(\bar{n}+1/2)\hbar\omega_o}{\epsilon_o V E_o^2 t_p} \tag{9}$$

Equation (9) can be written in a compact and more often used form since

$$Q = \frac{\omega_o}{\Delta\omega_c} = \frac{\omega_o \epsilon_o V E_o^2}{4P}$$

Here P is the power output of the cavity mode due to all loss mechanisms. Using this relation, Eq. (9) can be written as

$$\frac{\hbar\omega_o(\Delta\omega_c)^2}{2P}(\bar{n}+1/2). \tag{10}$$

The linewidth contribution from atoms inside the laser cavity is calculated in exactly the same way, except that in this case, the cavity mode is considered to be in equilibrium with two level atoms at a negative temperature $\bar{T}$ defined by the relationship

$$\frac{N_2}{N_1} = e^{\hbar\omega_o/k\bar{T}}$$

Here N_2 and N_1 are the number of atoms in the upper and lower atomic states respectively. As a result,

$$\bar{n}+1/2 = \frac{1}{e^{\frac{\hbar\omega_o}{kT}} - 1} + \frac{1}{2} = 1/2 \frac{N_2 + N_1}{N_2 - N_1}$$

so that the atoms inside the cavity contribute to the laser linewidth an amount

$$\frac{\hbar\omega_o}{2P}(\Delta\omega_c)^2\left(\frac{N_2 + N_1}{N_2 - N_1}\right)\frac{1}{2} \tag{11}$$

Finally, the total oscillation full linewidth is equal to the sum of these contributions. Therefore,

$$\Delta\omega_o = \frac{\hbar\omega_o(\Delta\omega_c)^2}{2P}\left[\bar{n}+1/2 + \frac{1}{2}\left(\frac{N_2 + N_1}{N_2 - N_1}\right)\right] \tag{12}$$

This result agrees with the linewidth expression derived by Scully and Lamb (1966).

The Feynman Path Integral Approach

An interesting approach for studying statistical problems is the Feynman path integral approach. Using this approach, it will be possible to derive Eq. (12) including some additional broadening due to saturation, amplitude noise, and atomic-line broadening.

This section is a summary of the Feynman path integral method. Although this approach is well known, the technique is not normally taught, so that this section is

included for completeness. The ideas presented here are found in complete form in Quantum Mechanics and Path Integrals by Feynman and Hibbs (1965). Since this approach is not the standard technique, it is reasonable to question its real utility. However, as expressed by Feynman and Hibbs in the last paragraph of their book:

> An effort to extend the path integral approach beyond its present limits continues to be a worthwhile pursuit; for the greatest value of this technique remains in spite of its limitations, i.e., the assistance which it gives to one's intuition in bringing together physical insight and mathematical analysis (p. 356).

The application of the technique to noise in laser oscillators is a small extension of these ideas.

The essential idea of an integral over all paths, a path integral, is presented in the context of quantum mechanics. Later in the section it will be applied to probability type problems.

Path Integrals and Quantum Mechanics

The essential ideas of the path integral technique can be gained by imagining a particle constrained to move in only one dimension. The position of the particle at any time can be specified by a coordinate x which is a function of time t. By a path then is meant a function x(t). In classical mechanics, if a particle at an initial time t_o, starts from a point x_o, and goes to a final point x_n at t_n, and if the force is deterministic, then there is

only one specific trajectory along which the particle can travel, the so called classical trajectory determined by a solution of Newton's second law and the boundary conditions. According to Feynman however, in quantum mechanics the motion of the particle can be interpreted in quite a different way. It is necessary to talk of the probability amplitude of an event. If an event can occur in several alternate but indistinguishable ways, then the overall probability amplitude for the event is obtained by adding the amplitudes for each alternative way. The probability that the event will happen is given by the absolute square of the overall amplitude. Alternative ways are said to be indistinguishable if at the end of the experiment it is not possible to tell which way the event occurred. Thus, if ϕ_1 and ϕ_2 represent the amplitudes for alternative ways an event can occur, the probability of the event, P, is given by the equation

$$P = |\phi_1 + \phi_2|^2$$

For the event, a particle travels from x_o at t_o to x_n at t_n, there are an infinite number of alternative paths x(t). These paths are indistinguishable because it is not possible to determine from the boundary conditions along which path the particle completed the event. The overall amplitude for the event is the sum of the amplitudes

for each of these infinity of alternative ways. Thus, if $\phi[x^i(t)]$ represents the amplitude that the particle took the path $x^i(t)$, and $K(x_n, t_n; x_o, t_o)$ the overall amplitude for the event, then

$$K(x_n, t_n; x_o, t_o) = \sum_{\substack{\text{all paths} \\ x^i(t)}} \phi[x^i(t)]$$

The essence of the path integral approach is contained in answers to the following two questions:

1. What is the amplitude for a particular path?
2. How is the sum accomplished?

The answer to question 1 requires a postulate equivalent to the statement of the Schrodinger equation: The contribution of a path has a phase equal to the action, S, divided by $\hbar$. The action is given by the expression

$$S = \int_{t_o}^{t_n} L(\dot{x}, x, t)\, dt$$

where L is the Lagrangian. Thus the amplitude for a path $x^i(t)$ is given by

$$\phi[x^i(t)] = \text{constant } e^{\frac{i}{\hbar}S[x^i(t)]}$$

The sum over all paths can be accomplished in the following way. The path is defined as a limit in which at first the path is only specified by giving its coordinate x

at a large number of specified times separated by very small intervals ϵ. The path sum is then an integral over all these coordinates. In order to complete the sum the limit is taken as ϵ approaches 0. This idea is shown in Fig. 4 taken from Feynman and Hibbs (1965).

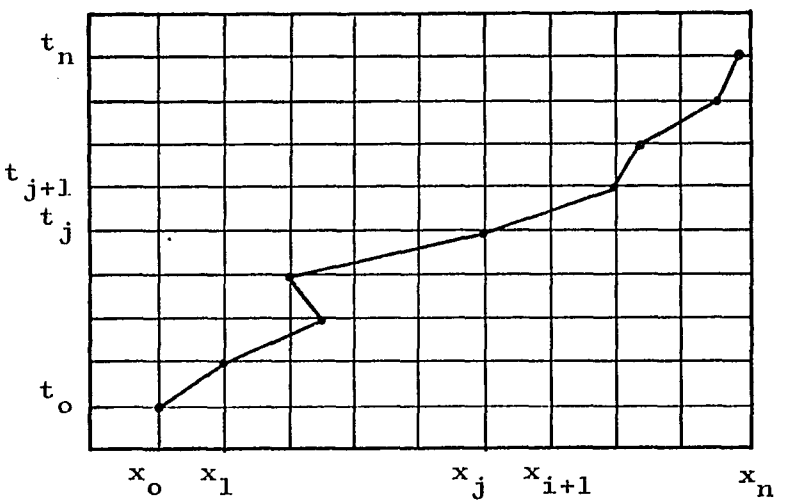

Fig. 4. A Particular Path x(t)

The overall amplitude, $K(x_n, t_n; x_o, t_o)$, covering all possible paths is then given by the following integral.

$$K(x_n,t_n;x_o,t_o) = \lim_{\epsilon \to 0} \int_{x_1} \int_{x_2} \cdots \int_{x_{n-1}} e^{\frac{i}{\hbar}S[x_n,t_n;x_o,t_o]} \frac{dx_1}{A} \frac{dx_2}{A} \cdots \frac{dx_{n-1}}{A} \qquad (13)$$

Here

$$S[x_n,t_n;x_o,t_o] = \int_{t_o}^{t_n} L(\dot{x},x,t)dt \tag{14}$$

is a line integral taken over the trajectory passing through the points x_j with straight lines in between. A is the normalizing constant. Equation (13) is written in a less restrictive notation as

$$K[N,O] = \int e^{\frac{i}{\hbar}S[N,O]} Dx(t)$$

and called a path integral.

There are several ways to perform the path integral and these will be described for a free particle. One way is to separate Eq. (14) in the following way,

$$S[N,O] = \int_{t_o}^{t_n} L(\dot{x},x,t)dt$$

$$= \int_{t_o}^{t_1} Ldt + \int_{t_1}^{t_2} dt + \ldots + \int_{t_{n-1}}^{t_n} Ldt \tag{15}$$

and then to approximate each integral of the sum by

$$\int_{t_j}^{t_{j+1}} L(\dot{x},x,t)dt = \varepsilon L\left(\frac{x_{j+1}-x_j}{\varepsilon}, \frac{x_j+x_{j+1}}{2}, \varepsilon\right) \tag{16}$$

For a free particle the Lagrangian is given by

$$L = \frac{m\dot{x}^2}{2}$$

and therefore, according to Eqs. (14), (15), and (16)

$$S[N,0] = \frac{m}{2} \sum_{i=1}^{N} \frac{(x_j - x_{j-1})^2}{\epsilon^2}$$

The overall amplitude for the event is then

$$K[N,0] = \lim_{\epsilon \to 0} \int_{x_1} \cdots \int_{x_{n-1}} \exp\left(\frac{i}{\hbar} \frac{m}{2\epsilon} \sum_{j=1}^{N} (x_j - x_{j-1})^2\right) \prod_{i=1}^{N-1} \frac{dx_i}{A} \tag{17}$$

The constant A can be determined in the following way. Notice that

$$K[N,0] = \lim_{\epsilon \to 0} \int_{x_{n-1}} \frac{dx_{n-1}}{A} e^{\frac{i}{\hbar} \frac{m(x_{n-1} - x_n)^2}{2\epsilon}} \left[\int_{x_1} \cdots \int_{x_{n-2}} e^{\frac{i}{\hbar} \frac{m}{2\epsilon} \sum_{j=1}^{n-1} (x_j - x_{j-1})^2} \prod_{i=1}^{n-2} \frac{dx_i}{A} \right]$$

$$= \lim_{\epsilon \to 0} \int_{x_{n-1}} \frac{dx_{n-1}}{A} e^{\frac{i}{\hbar} \frac{m}{2\epsilon} (x_n - x_{n-1})^2} K[N-1,0]$$

For this result to hold in the limit $\epsilon \rightarrow 0$

$$e^{\frac{i}{\hbar}\frac{m}{2\epsilon}(x_n - x_{n-1})^2} \longrightarrow \delta(x_n - x_{n-1})$$

Therefore,

$$\int_{-\infty}^{\infty} \frac{dx_{n-1}}{A}\, e^{\frac{i}{\hbar}\frac{m}{2\epsilon}(x_n - x_{n-1})^2} = 1$$

Upon integration this yields the constant

$$A = \sqrt{\frac{2\pi i\hbar\epsilon}{m}} \tag{18}$$

Using this result in Eq. (17), the integral is carried out on one variable after another. First carrying out the integration on x_1,

$$\int_{-\infty}^{\infty} \left(\frac{2\pi i\hbar\epsilon}{m}\right)^{-1/2} e^{\frac{i}{\hbar}\frac{m}{2\epsilon}[(x_2 - x_1)^2 + (x_1 - x_0)^2]}\, dx_1$$

$$= \left(\frac{2\pi i\hbar(2\epsilon)}{m}\right)^{-1/2} \exp\left[\frac{im}{2\hbar(2\epsilon)}(x_2 - x_0)^2\right]$$

Then the integration over x_2,

$$\int_{-\infty}^{\infty} dx_2 \left(\frac{2\pi i\hbar\epsilon}{m}\right)^{-1/2} \left(\frac{2\pi i\hbar\epsilon}{m}\right)^{-1/2} \exp\left\{\frac{im}{2\hbar(2\epsilon)}\left[(x_2 - x_0)^2 + 2(x_3 - x_2)^2\right]\right\} = \left(\frac{2\pi i\hbar(3\epsilon)}{m}\right)^{-1/2} \exp\left[\frac{im}{2\hbar(3\epsilon)}(x_3 - x_0)^2\right]$$

Continue this technique to x_{n-1} with the final result

$$K[N,0] = \lim_{\epsilon \to 0} \left(\frac{2\pi i\hbar(N\epsilon)}{m} \right)^{-1/2} \exp\left[\frac{im}{2\hbar(N\epsilon)} (x_n - x_0)^2 \right]$$

However,

$$N\epsilon = t_n - t_0 = T$$

so that

$$K[N,0] = \left(\frac{2\pi i\hbar T}{m} \right)^{-1/2} \exp\left[\frac{im}{2\hbar} \frac{(x_n - x_0)^2}{T} \right] \tag{19}$$

Gaussian Path Integrals

Although the above example illustrates a technique for calculating path integrals, there is another exact technique that is generally easier to use for actions, S, that involve the path $x(t)$, and $\dot{x}(t)$ up to and including the second power. Feynman and Hibbs (1965) call such path integrals Gaussian. These path integrals are interesting, not only because they include the solution of a wide variety of problems, but also because they illustrate the connection between classical and quantum mechanics.

The most general type of Lagrangian involving the path $x(t)$ to second order is written below:

$$L = a(t)\dot{x}^2 + b(t)\dot{x}x + c(t)x^2 + d(t)\dot{x} + e(t)x + f(t)$$

The action is the integral of this function between fixed end points. For this Lagrangian the amplitude that a

particle goes from x_a at t_a, to x_b at t_b, is given by the path integral taken over all possible paths.

$$K(b,a) = \int_a^b \exp\left[\frac{i}{\hbar}\int_{t_a}^{t_b} L(\dot{x},x,t)\right] Dx(t)$$

If $\bar{x}(t)$ denotes the classical path, it is an extremum for the action S. The action for the classical path is denoted by either $S_{c\ell}[b,a]$ or $S[\bar{x}(t)]$.

All paths from x_a to x_b can be covered by defining a point on the path by its distance from the classical path instead of its distance from an arbitrary coordinate axis. This is shown in Fig. 5, taken again from Feynman and Hibbs (1965).

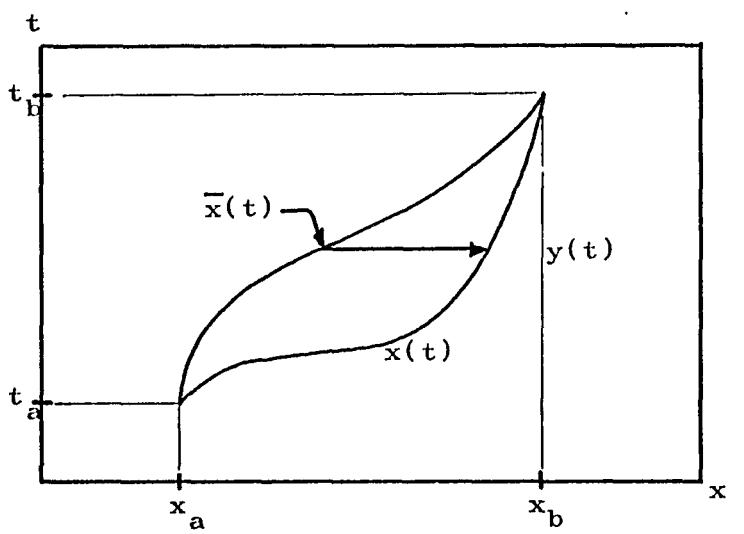

Fig. 5. Gaussian Method for Covering all Possible Paths

Here the arbitrary path x(t) is given by

$$x(t) = \bar{x}(t) + y(t)$$

and

$$S[x(t)] = S[\bar{x}(t) + y(t)]$$

$$= \int_{t_a}^{t_b} [a(t)(\dot{\bar{x}}^2 + 2\dot{\bar{x}}\dot{y} + \dot{y}^2) + \ldots]dt$$

$$= S_{c\ell}[b,a] + \int_{t_a}^{t_b} [a(t)\dot{y}^2 + b(t)\dot{y}y + c(t)y^2]dt \qquad (20)$$

This result follows since those terms that do not involve y(t) give the first term; those terms that involve y(t) and its derivative to first order give a vanishing contribution to the action since by Hamilton's principle the action is an extremum for the classical path, and

$$S[\bar{x}(t) + y(t)] - S[\bar{x}(t)] = 0$$

to first order in y(t). The last term in Eq. (20) is of the second order in y(t). Using Eq. (20) for the action, the amplitude can be written as shown below:

$$K[b,a] = e^{\frac{i}{\hbar}S_{c\ell}[b,a]} \int_0^0 \mathcal{D}y \exp\left\{\frac{i}{\hbar}\int_{t_a}^{t_b} [a(t)\dot{y}^2 + b(t)y\dot{y} + c(t)]\right\}$$

Because the end points x_a and x_b are specified, y(t) is zero at t_a and t_b, and the path integral can only be a

function of the times at the end points. Therefore,

$$K(b,a) = e^{\frac{i}{\hbar}S_{c\ell}[b,a]} F(t_a,t_b)$$

Thus, for quadratic Lagrangians, the amplitude for an event is determined by the classical action except for a function of the end points.

Consider again the simple example of a free particle where

$$L = \frac{m\dot{x}^2}{2}$$

The classical path is given by a solution of Lagrange's equation.

$$\frac{d}{dt}\left(\frac{\partial L}{\partial \dot{x}}\right) + \frac{\partial L}{\partial x} = 0$$

Then,

$$\ddot{x} = 0$$

and

$$\bar{x} = Ct + D$$

thus,

$$S_{c\ell} = \frac{m}{2}\int_{t_a}^{t_b} C^2 dt = \frac{m}{2}C^2(t_b - t_a)$$

Using the boundary conditions x_a at t_a, x_b at t_b,

$$C = \frac{x_b - x_a}{t_b - t_a}$$

and therefore,

$$S_{c\ell} = \frac{m}{2} \frac{(x_b - x_a)^2}{t_b - t_a}$$

so that

$$K[b,a] = e^{\frac{i}{\hbar} \frac{m}{2} \frac{(x_b - x_a)^2}{t_b - t_a}} F(t_a, t_b)$$

This is the same result as found by the technique leading to Eq. (19).

The reduction of a path integral to a differential equation can give $F(t_a, t_b)$ and also the usual differential equation formulation of a problem. For a free particle, reduction to differential form proceeds in the following way à la Feynman and Hibbs (1965).

Since the action is defined by an integral, the path integral can be split into two parts as shown in Fig. 6, and it can be expressed mathematically in the following way.

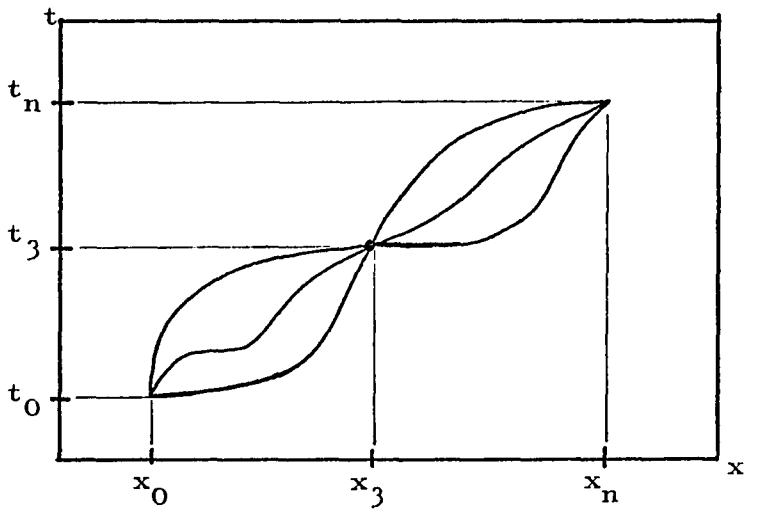

Fig. 6. Division of all Possible Paths into Two Groups

$$K[N,0] = \int\!\!\!\!\!\!\int e^{\frac{i}{\hbar}\int_{t_0}^{t_n} L\,dt}\, Dx(t)$$

$$= \int_{x_3} \int\!\!\!\!\!\!\int e^{\left[\frac{i}{\hbar}\int_{t_0}^{t_3} L\,dt + \frac{i}{\hbar}\int_{t_3}^{t_n} L\,dt\right]}\, Dx(t)\, dx_3$$

$$= \int_{x_3} \int\!\!\!\!\!\!\int e^{\frac{i}{\hbar}\{S[3,0] + S[N,3]\}}\, Dx(t)\, dx_3$$

$$= \int_{x_3} K[N,3]\, K[3,0]\, dx_3 \qquad (21)$$

Then, the wave function $\Psi(x_n,t_n)$ is defined as an amplitude to arrive at (x_n,t_n) from the past in some (perhaps unspecified) situation. When there is no point

in keeping track of where the particle came from, the wave function notation is used. Since a differential equation for the wave function is to be derived, Eq. (21) can be written as Eq. (22).

$$\Psi(x,t+\epsilon) = \int_{-\infty}^{\infty} K[x,t+\epsilon;\ y,t]\Psi(y,t)\ dy \tag{22}$$

Here the notation has been generalized to agree with Feynman and Hibbs (1965), and t_3 and t_n are assumed to differ only by an infinitesimal interval ϵ. Then,

$$\Psi[x,t+\epsilon] = \int_{-\infty}^{\infty} \frac{1}{A}\, e^{\frac{i}{\hbar}\int_y^x L(\dot{x},x,\epsilon)dt}\ \Psi(y,t)dy$$

$$= \int_{-\infty}^{\infty} \frac{1}{A}\, e^{\frac{i}{\hbar}\epsilon L\left(\frac{x-y}{\epsilon},\ \frac{x+y}{2}\right)}\ \Psi(y,t)dy$$

If L is the Lagrangian for a particle moving in a potential V(x,t) then it follows that

$$L = \frac{m\dot{x}^2}{2} - V(x,t)$$

and

$$\Psi(x,t+\epsilon) = \int_{-\infty}^{\infty} \frac{1}{A}\, \exp\left[\frac{i}{\hbar}\,\frac{m(x-y)^2}{2\epsilon}\right] \exp\left[-\frac{i}{\hbar}\,\epsilon V\left(\frac{x+y}{2},\ \epsilon\right)\right]$$

$$\Psi(y,t)dy \tag{23}$$

Because of the quantity $\frac{(x-y)^2}{\epsilon}$ in the exponential of the first term, the integral will be nearly zero unless y is near x. For this reason the integral can be expanded about x. Letting

$$y = x + \eta$$

$$dy = d\eta$$

Eq. (23) can be written as

$$\Psi(x,t) + \epsilon\frac{\partial\Psi}{\partial t} = \int_{-\infty}^{\infty} \frac{1}{A}\, e^{\frac{im\eta^2}{2\epsilon\hbar}}\left[1 - \frac{i\epsilon}{\hbar}\, V(x,t)\right]$$

$$\left[\Psi(x,t) + \eta\frac{\partial\Psi}{\partial x} + \frac{1}{2}\, y^2\, \frac{\partial^2\Psi}{\partial x^2}\right] d\eta$$

Taking the leading terms on both sides of this equality

$$1 = \frac{1}{A}\int_{-\infty}^{\infty} e^{i\frac{m\eta^2}{2\epsilon\hbar}}\, d\eta = \frac{1}{A}\left(\frac{2\pi i\hbar\epsilon}{m}\right)^{1/2}$$

so that

$$A = \left(\frac{m}{2\pi i\hbar\epsilon}\right)^{-1/2}$$

Equating and evaluating terms to first order in ϵ, the Schrodinger equation for a particle in one dimension is obtained:

$$-\frac{\hbar}{i}\frac{\partial\Psi}{\partial t} = -\frac{\hbar^2}{2m}\frac{\partial^2\Psi}{\partial x^2} + V(x,t)\Psi \qquad (24)$$

The technique for going from a path integral to a differential equation is useful, and it will be used later to derive the diffusion equation for the standing wave electric field of a laser oscillator.

A Path Integral Application in Optics

An interesting application of the path integral technique is to a derivation of the Fresnel diffraction integral.

A field component, u, of a single frequency light wave satisfies the scalar wave equation

$$\nabla^2 u + k^2 u = 0 \tag{25}$$

Here k is the propagation constant in the media. For light traveling in the z direction the field can be written as

$$u = \Psi(x,y,z)\exp(-ikz) \tag{26}$$

where Ψ is a slowly varying complex function which represents the difference between the wave under consideration and a plane wave. If Eq. (26) is used in Eq. (25), and it is assumed that Ψ varies so slowly with z that the second derivative $\frac{d^2\Psi}{dx^2}$ can be neglected, then Eq. (25) becomes

$$\frac{\partial^2\Psi}{\partial x^2} + \frac{\partial^2\Psi}{\partial y^2} - 2jk\frac{\partial\Psi}{\partial z} = 0 \tag{27}$$

This equation has the same form as Schrodinger's equation (Eq. 24) for a free particle in two dimensions. Letting $k = -\frac{m}{\hbar}$ the equations are equivalent. Thus, in analogy with Eq. (19), the propagation kernel for light from a point (x_1, y_1, z_1) to a point (x_2, y_2, z_2) is given by

$$K[x_2,y_2,z_2;x_1,y_1,z_1] = \frac{ik}{2\pi(z_2-z_1)} \exp\left[\frac{ik}{2}\frac{(x_2-x_1)^2 + (y_2-y_1)^2}{(z_2-z_1)}\right]$$

$$= \frac{i}{\lambda R} \exp\left\{\frac{i\pi}{\lambda R}[(x_2-x_1)^2 + (y_2-y_1)^2]\right\} \qquad (28)$$

In analogy with Eq. (22),

$$\Psi(x_2,y_2,z_2) = \int_{x_1}\int_{y_1} K[x_2,y_2,z_2;x_1,y_1,z_1] \Psi(x_1,y_1,z_1)dx,dy$$

$$= \frac{i}{\lambda R} \int_{-\infty}^{\infty}\int_{-\infty}^{\infty} e^{\frac{i\pi}{\lambda R}[(x_2-x_1)^2 + (y_2-y_1)^2]} \Psi(x_1,y_1,z_1)dx,dy$$

This is the Fresnel diffraction integral giving the amplitude distribution in one plane, if it is known in a previous plane.

The path integral interpretation of how light propagates from a plane z_1 to a plane z_2 is shown in Fig. 7. The classical, geometric optics path gives the

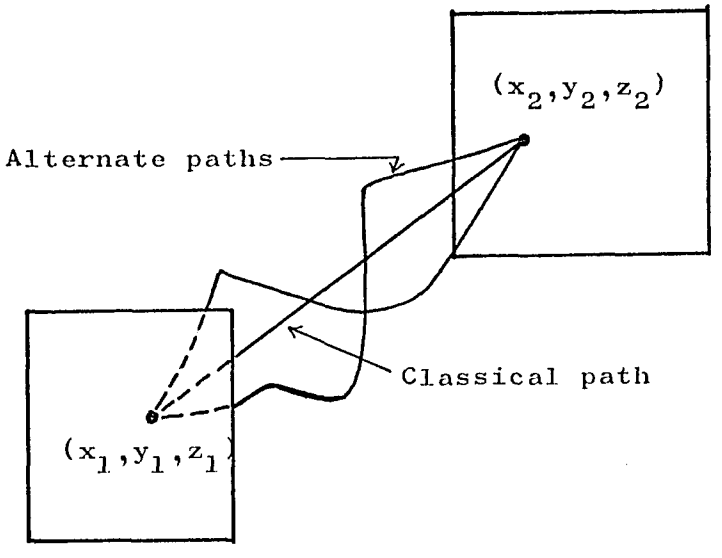

Fig. 7. Path Integral Interpretation of Light Propagation

main contribution to the propagation kernel, $e^{ikS_{c\ell}}$, while the other alternative paths contribute a factor that depends only on the position of the two end points.

Path Integrals in Probability

A classical type of probability problem involves a series of discrete events taking place at random times; for example, the spontaneous emission of photons by atoms in a resonant cavity. The photons are born at random times, but in any long time period T an average number $\bar{n}$ can be expected. In any actual measurement the exact number of photons born does not correspond to the expected number; however, the probability, P_n, that a particular

number are born during a period when the expected number is $\bar{n}$, is given by the Poisson distribution

$$P_n = \frac{\bar{n}^n}{n!e^{\bar{n}}} \tag{29}$$

For continuous variables, it is usual to denote the probability that a variable lies in a range dx about x by a continuous function P(x)dx. P(x) is the probability distribution of x, and the probability that x lies in the range x_a to x_b is given by

$$\int_{x_a}^{x_b} P(x)dx$$

Path integrals can be used in probability theory when the probability of obtaining a particular time history of a random phenomena is wanted; for example, the time history of the standing wave electric field in a laser cavity. That is, what is the probability of a function f(t)? If this probability is denoted by P[f(t)], then the probability of finding the function within a certain class of functions, for example, the class of functions with the same starting and ending values, can be written as a path integral

$$P[T|0] = \oint P[f(t)]Df(t)$$

In analogy to the mean value of a continuous variable, the mean value of a functional $Q[f(t)]$ is written

$$\langle Q \rangle = \frac{\int Q[f(t)]P[f(t)]Df(t)}{\int P[f(t)]Df(t)} \tag{30}$$

Of particular importance is the mean value of the exponential functional $\exp[ik(t)f(t)dt]$, defined to be the characteristic functional $\Phi[k(t)]$, where

$$\Phi[k(t)] = \frac{\int e^{i\int k(t)f(t)dt} P[f(t)]Df(t)}{\int P[f(t)]Df(t)} \tag{31}$$

Equation (31) is a path integral Fourier transform that can be inverted to give the probability functional as

$$P[f(t)] = \int e^{-i\int k(t)f(t)dt} \Phi[k(t)]Df(t)$$

A useful example is the characteristic functional of a function $f(t)$ that is not uncertain, but that is definitely known to be some function $F(t)$. That is

$$P[f(t)]Df(t) = \delta[f(t) - F(t)]Df(t)$$

so that the characteristic functional

$$\Phi[k(t)] = \int e^{i\int k(t)f(t)dt} \delta[f(t) - F(t)]Df(t)$$

$$= e^{i\int k(t)F(t)dt} \tag{32}$$

Some special properties of the characteristic functional are listed below:

$$\Phi[k(t)] = \frac{\int e^{i\int k(t)f(t)dt} P[f(t)]Df(t)}{\int P[f(t)]Df(t)} \tag{31}$$

$$\Phi[0] = 1 \tag{33}$$

$$\langle f(a)\rangle = -i \left.\frac{\delta\Phi[k(t)]}{\delta k(a)}\right|_{k(t)\,=\,0} \tag{34}$$

$$\langle f(a)f(b)\rangle = - \left.\frac{\delta^2\Phi[k(t)]}{\delta k(a)\ \delta k(b)}\right|_{k(t)\,=\,0} \tag{35}$$

In these properties $\left|\delta\Phi[k(t)]/\delta k(a)\right|\Big|_{k(t)\,=\,0}$ denotes the functional derivative of $\Phi[k(t)]$ with respect to the function $k(t)$ evaluated at $t = a$ and $k(t) = 0$.

It is often said that there are no new results that can be obtained from the path integral representation. Although this may be true, it is an alternate way to obtain useful results, and can thus add different insights from other techniques. This section has been a summary of some of the techniques and examples presented in Quantum Mechanics and Path Integrals by Feynman and Hibbs (1965). In the next section they will be used to more completely study laser oscillator phase noise.

Path Integral Description of Laser Oscillator Phase Noise

In this section phase fluctuations caused by random photons are described by using the path integral technique. Examination of the model for random phase photon noise, Fig. 3, shows that a particular time history of the

instantaneous phase can be written in the following way,

$$\phi(t) = \omega_o t + \sum_j \delta\phi_j u(t-t_j) \tag{36}$$

Here $u(t-t_j)$ represents a unit step function

$$u(t-t_j) = \begin{cases} 1 & t > t_j \\ 0 & t < t_j \end{cases}$$

The instantaneous frequency, $\dot{\phi}$, is given by

$$\dot{\phi} = \omega_o + \sum_j \delta\phi_j \delta(t-t_j) \equiv \omega_o + f(t) \tag{37}$$

Here, $\delta\phi_j$, is the step size of the phase step at t_j, and $\delta(t-t_j)$ is a Dirac delta function. The random properties of the phase are contained in the function f(t). This randomness is described by the characteristic functional, $\Phi[k(t)]$.

To aid in finding the characteristic functional, consider a time interval, T, during which N random phase events occur at times t_1, $t_2 \cdots t_n$. The complete history of the noise source, f(t), is

$$f(t) = \sum_{j=1}^{N} \delta\phi_j \delta(t-t_j)$$

If all times t_j and step sizes $\delta\phi_j$ are assumed known, then this is a statement of certainty, and according to Eq. (32) the characteristic functional is written as

$$\Phi_o[k(t)] = e^{i\int_0^T k(t) \sum_{j=1}^{N} \delta\phi_j \delta(t-t_j)dt} \tag{38}$$

However, it is more realistic to make the following assumptions:

1. The step sizes $\delta\phi_j$ are described by a probability distribution function, $p(\delta\phi_j)$, or by a corresponding characteristic function, $W(\omega)$. These are related in the usual way by Fourier transforms.

$$W(\omega) = \int_{\text{all } \delta\phi_j} e^{i\omega\delta\phi_j} p(\delta\phi_j) d(\delta\phi_j) \tag{39}$$

2. The times of photon birth are distributed uniformly over the interval T, so that the probability of a birth in time dt is dt/T.
3. The number of births, N, in a time, T, is given by the Poisson distribution

$$P_N = \frac{\bar{m}^N}{N! e^{\bar{m}}} \tag{40}$$

Here $\bar{m} = \mu T$, and μ is the mean rate at which photons are born. From the discussion of frequency fluctuations, this rate is

$$\mu = \left[(\bar{n} + \frac{1}{2}) + \frac{1}{2} \left(\frac{N_2 + N_1}{N_2 - N_1} \right) \right] \frac{1}{t_{\text{photon}}} \tag{41}$$

Using these assumptions a new characteristic functional, $\Phi_1[k(t)]$, is written as an average of $\Phi_o[k(t)]$ with respect to step sizes, $\delta\phi_j$, and times t_j.

$$\Phi_1[k(t)] = \int_0^T \cdots \int_{\text{all } \delta\phi_j} \Phi_o[k(t)] \prod_1^N P(\delta\phi_j)d(\delta\phi_j) \prod \frac{dt_j}{T}$$

$$= \int_0^T \cdots \int_{\text{all } \delta\phi_j} \exp\left\{ i \sum_{j=1}^N \int_0^T k(t)\delta\phi_j \delta(t-t_j)dt \right\}$$

$$\prod_1^N p(\delta\phi_j)d(\delta\phi_j) \prod \frac{dt_j}{T}$$

$$= \left(\int_0^T \int_{\text{all } \delta\phi_j} \exp\left\{ i \int_0^T k(t)\delta\phi_j \delta(t-t_j)dt \right\} p(\delta\phi_j) \right.$$

$$\left. d(\delta\phi_j) \frac{dt_j}{T} \right)^N$$

$$= \left(\int_0^T \int_{\text{all } \delta\phi_j} \exp\{ik(t)\delta\phi_j\} p(\delta\phi_j)d(\delta\phi_j) \frac{dt_j}{T} \right)^N$$

$$= \left(\int_0^T W[k(t_j)] \frac{dt_j}{T} \right)^N \equiv [A]^N \qquad (42)$$

In this expression W is the characteristic function defined in Eq. (39). If there were exactly N births in time T, $\Phi_1[k(t)]$ would be the desired characteristic functional. However, according to assumption 3 the number of births are Poisson distributed. Averaging (Eq. 42) with

respect to the number of random phase photon births in time T leads to the result

$$\Phi_2[k(t)] = \sum_N \Phi_1[k(t)] \frac{\bar{m}^N}{N!} e^{-\bar{m}}$$

$$= \sum_N [A]^N \frac{\bar{m}^N}{N!} e^{-m} = e^{A\bar{m}-\bar{m}}$$

$$= e^{\bar{m}\left[\int_0^T W[k(t_j)] \frac{dt_j}{T} - 1\right]} \tag{43}$$

The characteristic function, $W[k(t_j)]$, is approximated in the following way:

$$W[k(t)] = \int p(\delta\phi_j)\, e^{ik(\delta\phi_j)}\, d(\delta\phi_j)$$

$$= \int p(\delta\phi_j)\left[1 - k(\delta\phi_j) + \frac{k^2}{2}(\delta\phi_j)^2 \ldots\right] d(\delta\phi_j)$$

$$= 1 - k\langle\delta\phi_j\rangle + \frac{k^2}{2}\langle(\delta\phi_j)^2\rangle + \ldots$$

From the model for photon noise, Fig. 3,

$$\langle\delta\phi_j\rangle = 0$$

and

$$\langle(\delta\phi_j)^2\rangle = \frac{2\hbar\omega}{\epsilon_o V E_o^2}$$

Assuming that the mean squared step size is small, only terms through second order need be kept; Eq. (43) then becomes

$$\Phi_2[k(t)] = \exp\left\{-\mu T\left[\int_0^T \left(1 + \frac{k(t_j)^2}{2}\right)\langle(\delta\phi_j)^2\rangle \frac{dt_j}{T} - 1\right]\right\}$$

$$= \exp\left[-\frac{1}{2}\mu\langle(\delta\phi_j)^2\rangle \int_0^T k(t)^2 dt\right] \qquad (44)$$

The Fourier inverse of Eq. (44) gives the probability functional of the noise source f(t) as

$$P[f(t)]Df(t) = \exp\left\{\frac{-\frac{1}{2}\int_0^T [f(t)]^2 dt}{\mu\langle(\delta\phi_j)^2\rangle}\right\} Df(t) \qquad (45)$$

This result shows how a shot noise type process can lead to a Gaussian noise type functional. In addition, comparison of Eq. (44) and Eqs. (12-40) of Feynman and Hibbs (1965) which gives the most general form of a Gaussian characteristic functional as

$$\Phi = \exp\{i\int k(t)F(t)dt - \frac{1}{2}\int k(t)k(t')A(t,t')dtdt'\}$$

where $\langle f(t)\rangle = F(t)$

and $\langle f(t)f(t')\rangle = A(t,t')$

shows that the correlation function of the noise source f(t) is given by

$$A(t,t') = \langle f(t)f(t')\rangle = \mu\langle(\delta\phi_j)^2\rangle\delta(t-t') = A(t-t')$$

$$= \frac{2\hbar\omega}{\epsilon_o V E_o^2}\left[(\bar{n}+\frac{1}{2}) + \frac{1}{2}\left(\frac{N_2+N_1}{N_2-N_1}\right)\right]\frac{1}{t_p}\,\delta(t-t')$$

$$= D\delta(t-t')$$

In this case the noise source is delta function correlated.

Since the relationship, Eq. (37), between the phase and the force is linear, the probability functional of ϕ can be found from Eq. (45) by a change of variable. Thus,

$$P[\phi(t)]D\phi(t) = P[f(t)]Df(t)$$

$$= K' \exp\left\{\frac{-\frac{1}{2}\int_0^T (\dot{\phi}-\omega_o)^2 dt}{\mu\langle(\delta\phi_j)^2\rangle}\right\} D\phi(t) \qquad (46)$$

Here K' is a normalization constant.

A function of more interest is the probability that the phase at time τ is $\phi(\tau)$, if at time $t = 0$ it was $\phi(0)$. This is the ordinary conditional probability function $P\left|\phi(\tau)\,|\phi(0)\right|$. Since there are many paths connecting these end conditions, $P\left|\phi(\tau)\,|\phi(0)\right|$ is the path integral of Eq. (37) over all paths between $\phi(0)$ and $\phi(\tau)$. Therefore,

$$P\left|\phi(\tau)\,|\phi(0)\right| d\phi_\tau = \left(\int_{\phi(0)}^{\phi(\tau)} K' \exp\left\{-\frac{1}{2}\int_0^\tau \frac{(\dot{\phi}-\omega_o)^2 dt}{D}\right\} D\phi(t)\right) d\phi_\tau \qquad (47)$$

Equation (47) is a Gaussian path integral that can be solved by the classical path technique so that

$$P\left|\phi(\tau)\,|\phi(0)\right| d\phi_\tau = Ke^{E_{c\ell}} d\phi_\tau$$

where $E_{c\ell} = \int_0^\tau "L_{c\ell}"\, dt$

and $L_{c\ell} = (\dot{\phi}_{c\ell} - \omega_o)^2$ (48)

The classical path is defined by solution of Eq. (49)

$$\frac{d}{dt}\left(\frac{\partial L}{\partial \dot{\phi}}\right) - \frac{\partial L}{\partial \phi} = 0 \qquad (49)$$

with the boundary conditions

$$\phi(t=0) \equiv \phi(0)$$

$$\phi(t=\tau) \equiv \phi(\tau)$$

The solution of Eq. (49) is

$$\phi_{c\ell}(t) = \frac{\phi(\tau) - \phi(0)}{\tau}\, t + \phi(0) \equiv At + \phi(0)$$

so that

$$\dot{\phi}_{c\ell} - \omega_o = A - \omega_o$$

and $E_{c\ell} = \int_0^\tau L_{c\ell}\, dt = \int_0^\tau (\dot{\phi}_{c\ell} - \omega_o)^2\, dt$

$$= \left[\left|\phi(\tau) - \phi(0)\right| - \omega_o\tau\right]^2 \frac{1}{|\tau|}$$

Hence,

$$P\left|\phi(\tau)\,|\phi(0)\right| d\phi_\tau = C \exp\left\{-\frac{1}{2}\frac{\left[\left|\phi(\tau)-\phi(0)\right| - \omega_o\tau\right]^2}{D|\tau|}\right\} d\phi_\tau \tag{50}$$

This is a Gaussian probability function with the properties

$$\langle \phi(\tau) - \phi(0)\rangle = \omega_o\tau$$

$$\langle \left|\phi(\tau) - \phi(0)\right|^2\rangle = D|\tau|$$

The magnitude signs on τ are used since $\langle \left|\phi(\tau) - \phi(0)\right|^2\rangle$ must be positive. The steps leading to the laser linewidth are the same as those from Eq. (1) to Eq. (4).

The technique for finding the conditional probability $P\left|\phi(t)\,|\phi(0)\right|$, Eq. (50), is equivalent to solving the diffusion equation. This can be shown by deriving a differential equation from the path integral Eq. (47) in a way analogous to the derivation of Schrodinger's equation from a path integral.

Change variables in Eq. (47) to

$$\oint = \Phi - \omega_o t$$

$$\dot{\oint} = \dot{\Phi} - \omega_o$$

so that Eq. (47) becomes

$$P(\phi_\tau, t\,|\,\phi_o, 0)\,d\phi_\tau = \left[\int K' \; e^{-\frac{1}{2D}\int_0^\tau \dot{\phi}^2 dt}\; D\phi(t)\right] d\phi_\tau$$

$$= \lim_{\epsilon\to 0} \int e^{-\frac{1}{2D}\sum_{i=1}^{\tau}\left(\frac{\phi_i-\phi_{i-1}}{\epsilon}\right)^2} \epsilon \prod_{i=1}^{\tau-1} \frac{d\phi_i}{A}\, d\phi_\tau$$

$$= \lim_{\epsilon\to 0} \int \left(e^{-\frac{1}{2D\epsilon}\sum_{i=1}^{\tau-1}(\phi_i-\phi_{i-1})^2} \prod_{i=1}^{\tau-2} \frac{d\phi_i}{A} \right) \left(e^{-\frac{1}{2\epsilon D}(\phi_\tau-\phi_{\tau-1})^2} \frac{d\phi_{\tau-1}}{A} \right) d\phi_\tau$$

$$= \lim_{\epsilon\to 0} \left(\int P(\phi_{\tau-1}, \tau-1\,|\,\phi_o, 0)\; e^{-\frac{1}{2\epsilon D}(\phi_\tau-\phi_{\tau-1})^2} \frac{d\phi_{\tau-1}}{A} \right) d\phi_\tau$$

As $\epsilon \to 0$ $\quad \dfrac{e^{-\frac{1}{\epsilon D}\frac{(\phi_\tau-\phi_{\tau-1})^2}{}}}{A} \longrightarrow \delta(\phi_{\tau-1} - \phi_\tau)$

so that

$$\int \exp\left[-\frac{(\phi_\tau-\phi_{\tau-1})^2}{2\epsilon D}\right] \frac{d\phi_{\tau-1}}{A} = 1$$

Therefore,

$$A = \sqrt{2\pi\epsilon D}.$$

Using the amplitude multiplication rule Eq. (21) for this path integral, and incrementing τ by ϵ, gives

$$P(\phi_\tau, \tau | \phi_o, 0) d\phi_\tau = \int P(\phi_\tau, \tau | \phi_{\tau-\epsilon}, \tau-\epsilon) P(\phi_{\tau-\epsilon}, \tau-\epsilon | \phi_o, 0)$$

$$\frac{d\phi_{\tau-\epsilon} d\phi_\tau}{A}$$

$$= \int P(\phi_{\tau-\epsilon}, \tau-\epsilon | \phi_o, 0) \; e^{-\frac{1}{2} \frac{(\phi_\tau - \phi_{\tau-\epsilon})^2}{\epsilon D}} \frac{d\phi_{\tau-\epsilon} d\phi_\tau}{A}$$

Letting

$$\phi_\tau - \phi_{\tau-\epsilon} = u,$$

then

$$P(\phi_\tau, \tau | \phi_o, 0) d\phi_\tau = \int_{-\infty}^{\infty} P(\phi_\tau - u, \tau-\epsilon | \phi_o, 0) \; e^{-\frac{1}{2} \frac{u^2}{\epsilon D}} \frac{du}{A} \, d\phi_\tau$$

so that expanding each side in small parameters ϵ and μ,

$$\left(P(\phi_\tau, \tau-\epsilon | \phi_o, 0) + \epsilon \frac{\partial P}{\partial t} + \cdots \right) d\phi_\tau$$

$$= \int_{-\infty}^{\infty} \left[P(\phi_\tau, \tau-\epsilon | \phi_o, 0) - u \frac{\partial P}{\partial \phi} + \frac{u^2}{2} \frac{\partial^2 P}{\partial \phi^2} \right] e^{-\frac{1}{2} \frac{u^2}{\epsilon D}} \frac{du}{A} \, d\phi_\tau$$

$$= \left(P - \frac{\partial P}{\partial \phi} \int_{-\infty}^{\infty} u \; e^{-\frac{1}{2} \frac{u^2}{\epsilon D}} \frac{du}{A} + \frac{1}{2} \frac{\partial^2 P}{\partial \phi^2} \int_{-\infty}^{\infty} u^2 \; e^{-\frac{1}{2} \frac{u^2}{\epsilon D}} \frac{du}{A} \right) d\phi_\tau$$

Carrying out the integrations, comparing terms of the first order of ϵ, and letting $\epsilon \to 0$ in the argument, we find that

$$\frac{\partial P}{\partial t} = \frac{D}{2} \frac{\partial^2 P}{\partial \phi^2} \tag{51}$$

Equation (51) is the diffusion equation. Its solution would also lead to the result Eq. (50).

So far an expression for the oscillation linewidth has been obtained only for the case where the cavity frequency is equal to the atomic-line center frequency. There are additional fluctuations caused by coupling of the field amplitude into the frequency equation (Eq. 37) when the oscillator is detuned from atomic line center. According to Lamb (1964), the frequency of a single mode laser detuned from atomic line center is determined by the following equation

$$\dot{\phi} = \omega_c + \sigma + \rho E^2 \tag{52}$$

Here ω_c is the empty cavity resonant frequency and σ and ρ are constant functions depending on the difference between ω_c and the atomic center frequency, ω_a.

If the laser is operating far enough above threshold, the field can be approximated by a constant term E_o plus a fluctuating field e(t) determined by random noise. The constant field E_o is determined by the stationary solution of Lamb's amplitude equation

$$\dot{E} = \alpha E - \beta E^3 \tag{53}$$

In the steady state

$$\dot{E} = 0$$

so that

$$E_o = \sqrt{\frac{\alpha}{\beta}}$$

and

$$E = E_o + e(t) \tag{54}$$

When Eq. (54) is substituted into Eq. (52)

$$\dot{\phi} = \omega_c + \sigma + \rho E_o^2 + 2\rho E_o e(t) \tag{55}$$

The first three terms lead to a new oscillation frequency depending on $\omega_c - \omega_a$ and replace ω_o of the previous analysis as the average frequency. The additional term, $2\rho E_o e(t)$, gives frequency fluctuations caused by amplitude noise. These additional fluctuations can be included in the previous analysis.

According to the laser noise model, Fig. 3, the fluctuating field e(t) is given by the sum of a series of jumps caused by the spontaneous emission noise process. Each of these small amplitude jumps, $\Delta E_{\parallel j}$, decay according to Eq. (52) with

$$E = E_o + \Delta(t_j)$$

so that

$$\dot{\Delta} + 2\beta E_o^2 \Delta = 0$$

and therefore,

$$\Delta = \Delta E_{\|j}\, e^{-2\beta E_o^2 (t-t_j)}$$

Normally

$$2\beta E_o^2 >> \frac{1}{tp}$$

so that one amplitude jump has decayed away before another one occurs, and $\exp(-2\beta E_o^2 t)$ may be approximated by a delta function of amplitude $\frac{1}{2\beta E_o^2}$. Hence,

$$\Delta = \frac{\Delta E_{\|j}}{2\beta E_o^2}\, \delta(t-t_j) \tag{56}$$

The time history of the amplitude fluctuations, $e(t)$, is then given by the sum

$$e(t) = \sum_j \frac{\Delta E_{\|j}}{2\beta E_o^2}\, \delta(t-t_j) \tag{57}$$

The phase equation (Eq. 55) including $f(t)$ of the previous analysis then becomes

$$\dot{\phi} = \omega_c + \sigma + \rho E_o^2 + \frac{\rho}{\beta E_o} \sum_j \Delta E_{\|j}\, \delta(t-t_j) + \sum_j \delta\phi_j \delta(t-t_j)$$

$$\equiv \omega_o' + \sum_j \left(\frac{\rho}{\beta E_o} \Delta E_{\|j} + \delta\phi_j\right) \delta(t-t_j)$$

This equation is of the same form as Eq. (37), and according to Eq. (46), the laser linewidth is

$$D = \Delta\omega_o = \mu\langle(\frac{\rho}{\beta E_o}\Delta E_{\parallel j} + \delta\phi_j)^2\rangle$$

$$= \mu[(\frac{\rho}{\beta E_o})^2\langle(\Delta E_{\parallel j})^2\rangle + \langle(\delta\phi_j)^2\rangle]$$

since

$$\langle\Delta E_{\parallel j}\delta\phi_j\rangle = \langle(\frac{\hbar\omega}{\varepsilon_o V E_o})\sin\theta_i\cos\theta_i\rangle = 0$$

Since

$$\Delta E_{\parallel j} = 2(\frac{\hbar\omega}{\varepsilon_o V})^{1/2}\cos\theta_i$$

and

$$p(\theta_i)d\theta_i = \frac{1}{2\pi}d\theta_i$$

Then $$\langle(\Delta E_{\parallel j})^2\rangle = \frac{2\hbar\omega}{\varepsilon_o V}$$

Therefore,

$$\Delta\omega_{osc} = \mu[(\frac{\rho}{\beta})^2 + 1]\frac{2\hbar\omega}{\varepsilon_o V E_o^2}$$

$$= \frac{\hbar\omega(\Delta\omega_c)^2}{2P}[(\bar{n} + \frac{1}{2}) + \frac{1}{2}(\frac{N_2+N_1}{N_2-N_1})]\left(1 + (\frac{\rho}{\beta})^2\right) \qquad (58)$$

The factor $\frac{\rho}{\beta}$ is given by Lamb (1964) as

$$\frac{\rho}{\beta} = \frac{\Delta\omega_c}{2\beta E_o^2}\left\{\left[\frac{Z_i(\omega_c-\omega_a)}{Z_i(0)}\right]\eta-1\right\}\left\{\frac{\gamma_{ab}(\omega_c-\omega_a)}{2\gamma_{ab}^2+(\omega_c-\omega_a)^2}\right\}$$

The function Z_i is the plasma dispersion function, η is the relative excitation, and $\gamma_{ab} = \frac{1}{2}(\gamma_a+\gamma_b)$ is the average of the decays constants of the upper and lower laser levels.

Equation (58) represents the final expression for the laser oscillation linewidth including the effects of atomic-line broadening and saturation.

A treatment of amplitude noise in a laser oscillator can also be formulated in terms of path integrals in a similar way by starting with Lamb's amplitude equation and using the noise model, Fig. 3.

In summary, it has been possible using Feynmann path integral techniques, to start with a simple model and derive all of the statistical properties of the standing wave field phase. Included are the following facts: the driving noise force is delta function correlated (Eq. 46) with statistical properties described by a Gaussian distributional (Eq. 45); the force leads to a Gaussian distribution function for accumulated phase (Eq. 50) that obeys the diffusion equation (Eq. 51); the effects of atomic line-broadening and saturation on the oscillation linewidth can be easily included (Eq. 58).

CHAPTER III

EXPERIMENT

Design Philosophy

This chapter presents some of the design philosophy, method of measurement, some experimental results, and a description of the equipment used to directly measure the oscillation linewidth of a 3.39μ He-Ne laser. Table 1 gives a summary of factors considered in the design. Chapter IV describes the results.

As has already been described, phase fluctuations due to spontaneous emission are the predominant contributor to the power spectrum of the total field. However, these fluctuations are difficult to measure because they can be so easily masked by the effects of man-made disturbances. The difficulty arises because the laser linewidth, $\Delta\nu_o$, is usually narrow, while the operating frequency of the laser is very sensitive to cavity length changes. For example, a 10 cm, 3.39μ, He-Ne laser with a 10 MHz cavity full width and a power output of 1μ watt has an oscillation linewidth of approximately 20 Hz. If for some reason the cavity length changes by 1A°, the laser center frequency changes approximately 100 KHz ($\Delta\nu = \nu\frac{\Delta L}{L}$)--very small random jumps easily mask a few Hertz laser linewidth caused by quantum

Table 1. Influences That Can Cause Undesirable Noise and Precautions Taken to Reduce Their Effect

Considerations	Precautions
1. Make $\Delta\nu_o$ broader than the spectrum analyzer instrument resolution	1. a. Make P small b. Make $\Delta\nu_c$ large $(\Delta\nu_o = \frac{\pi h\nu(\Delta\nu_c)^2}{P})$
2. Reduce the influence of environmental disturbances	2. a. Dual-laser design b. Use acoustical shielding and mechanical isolation c. Optically contact all elements
3. Length fluctuations caused by thermal fluctuations of lowest order mechanical mode of quartz block	3. Too small to be of importance
4. Power supply instabilities	4. a. Add additional filtering to power supplies b. Operate lasers near current saturation c. Operate lasers near line center d. Operate both laser power supplies from the same crystal oscillator
5. Tuning cell pressure fluctuations	5. a. Use good vacuum techniques b. Reduce the tuning cell volume
6. Detector and lens feedback	6. Tip elements slightly off beam axis
7. Noise caused by combining optics jitter	7. Use special beam splitter mirror element
8. Plasma noise	8. Use r-f excitation

noise. Mechanical and acoustical noise in an ordinary laboratory easily cause frequency jumps of this order in all but the most carefully designed lasers. In fact, in the first attempt to measure laser frequency stability, Javan, Ballik, and Bond (1962) were hampered by frequency jumps of just this order of magnitude. It is no wonder that their next attempt was made in an isolated wine cellar. In that quiet environment, they reported an improvement of stability of about a factor 10^4 compared to their previous results.

In the design of our experiment to measure oscillation linewidth, we had two primary objectives:

1. To offset the effects of acoustical and mechanical noise by making them, as nearly as possible, the same for two lasers.
2. To increase the oscillation linewidth so that it is not easily masked by disturbances that are not the same for the nearly identical lasers.

The first objective was accomplished by building two lasers in a single quartz block, a dual-laser design, shown in Fig. 8. The second was accomplished by designing a laser oscillator with a large cavity bandwidth, $\Delta\nu_c$, and small power output, P. This is desirable because the oscillation linewidth is essentially given by the expression

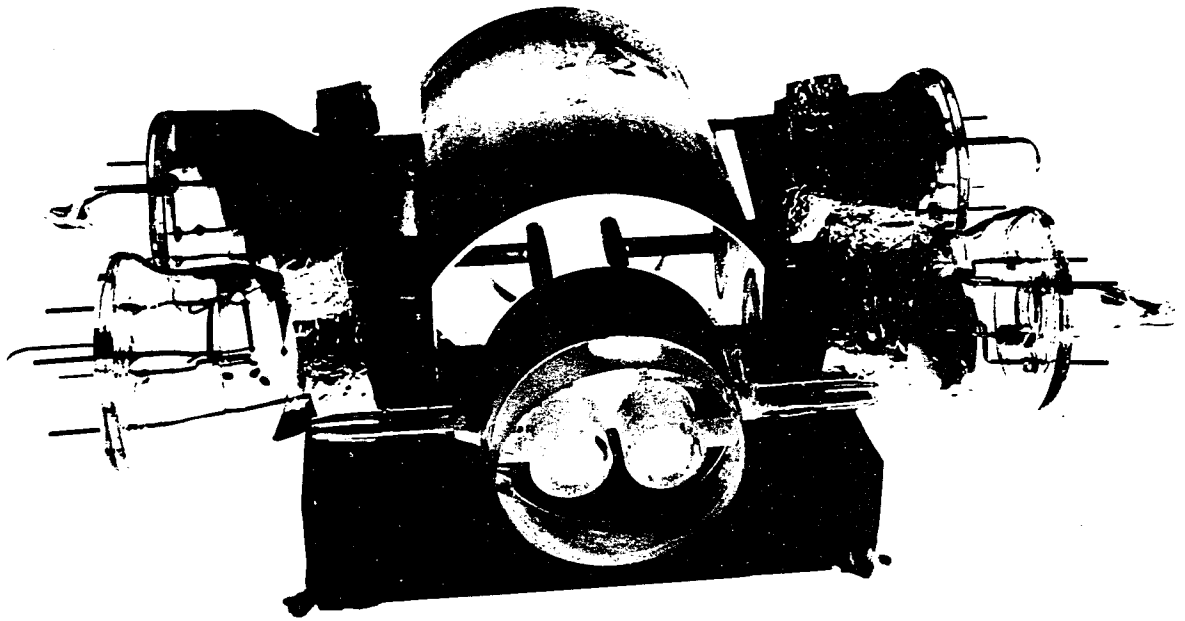

Fig. 8. The Dual Laser

$$\Delta\nu_{osc} = \frac{\pi h\nu(\Delta\nu_{cav})^2}{P} \tag{59}$$

The experimental arrangement shown in Fig. 9 was used to observe the beat frequency between the two laser light outputs from the dual laser, Fig. 8. We show in Appendix A that the spectrum of the beat note displayed by the spectrum analyzer is proportional to the spectral density of the phase, $S_{\phi}(\omega)$, convolved with the spectrum analyzer resolution.

General Design Considerations

The Laser

The requirement that the oscillation linewidth be large compared to the broadening effects of cavity vibration was a primary consideration in deciding upon the laser transition to be used in the experiment. A meaningful figure of merit is the ratio of the oscillation linewidth, $\Delta\nu_o$, to the frequency change, $\Delta\nu_L$, caused by a cavity length change ΔL. Thus,

$$f \equiv \frac{\Delta\nu_o}{\Delta\nu_L}$$

$$= \frac{\pi h\nu(\Delta\nu_c)^2}{P(\frac{\Delta L}{L})\nu} \tag{60}$$

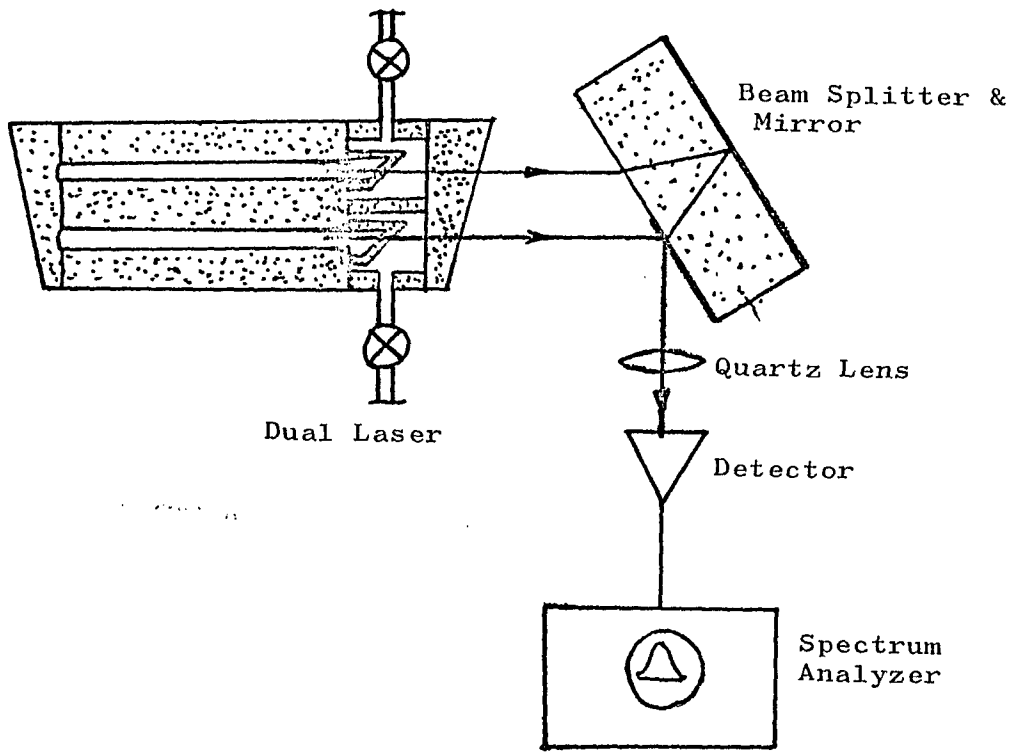

Fig. 9. Arrangement for Laser Linewidth Measurement

If it is assumed that the laser transitions to be considered are essentially inhomogeneously broadened, the lasers are operated single frequency at line center, and that they are all the same amount above threshold, then the power outputs can be expressed as (Bell and Sinclair, 1969)

$$P = \frac{w_o(1-R)}{2}\left(\left(\frac{g_oL}{1-R}\right)^2 - 1\right)$$

$$= k\, w_o(1-R)$$

Here k is a constant and w_o is the saturation parameter. The excitation parameter, $g_oL/(1-R)$, is assumed constant since all lasers are assumed to be operated the same amount above threshold. With these assumptions, the figure of merit can be rewritten as

$$f = \frac{\pi h\nu(\Delta\nu_c)^2}{P(\frac{\Delta L}{L})\nu}$$

$$= \frac{\pi h[\frac{1}{\pi}\frac{c}{2L}(1-R)]^2}{k\, w_o(1-R)(\frac{\Delta L}{L})}\left(\frac{g_oL}{g_oL}\right)$$

$$= \left(\frac{hc^2}{4\pi k\Delta L}\right)\left(\frac{1-R}{g_oL}\right)\left(\frac{g_o}{w_o}\right)$$

$$= K\left(\frac{g_o}{w_o}\right) \qquad (61)$$

We define a new figure of merit

$$F = \frac{g_o}{w_o} \tag{62}$$

A large figure of merit, F, is desirable. Therefore, the best system has a large small signal gain and a small saturation parameter. Because we had some experience at building He-Ne lasers, these were the primary ones considered. Listed below are figures of merit for the 3 most common He-Ne laser transitions:

$.6328\mu$ $\quad F = \frac{g_o}{w_o} = 10^{-2} \frac{\text{db-cm}}{\text{watt}}$

1.15μ $\quad F = 5 \times 10^{-2} \frac{\text{db-cm}}{\text{watt}}$

3.39μ $\quad F = 26 \frac{\text{db-cm}}{\text{watt}}$

The 3.39μ He-Ne laser has the highest figure of merit. For this reason, and because of the interest in the 3.39μ transition as a frequency standard, it was chosen for study.

The Dual Laser Structure

In order to measure oscillation linewidth caused by quantum noise, special techniques were needed to minimize the masking effects of man-made disturbances. These disturbances were reduced by working on a granite slab that floats on air cushions, enclosing the lasers inside an

acoustical shield, and working in the dead of night. However, even with these precautions, the remaining disturbances affect individually designed lasers differently enough to broaden the beat note spectrum and mask the narrow quantum noise spectral profile. With these ideas in mind, Dr. Roland Shack of the Optical Science Department suggested that we consider a dual-laser-type design. In this design, both lasers are built into a single quartz block with mirrors and Brewster windows optically contacted to the block to give the structure maximum stability and mechanical integrity (Fig. 8). The intention of this design is to make both lasers have identical cavity vibrations due to man-made disturbances, so that the beat frequency between the two lasers is relatively free of the effects of the environment. Quantum noise effects, which are independent in each laser, then become apparent. One of the important results of the experiment was to see how well this type of structure accomplished its purpose. A typical beat frequency spectrum is shown in Fig. 10. This picture was taken from a spectrum analyzer display when both lasers were operating well above threshold. The dual laser was floated on a granite slab, acoustically shielded with a plywood box, a 2" layer of fiberglass, some lead, and another 2" layer of fiberglass. All electronic equipment was removed from the basement room of the Optical

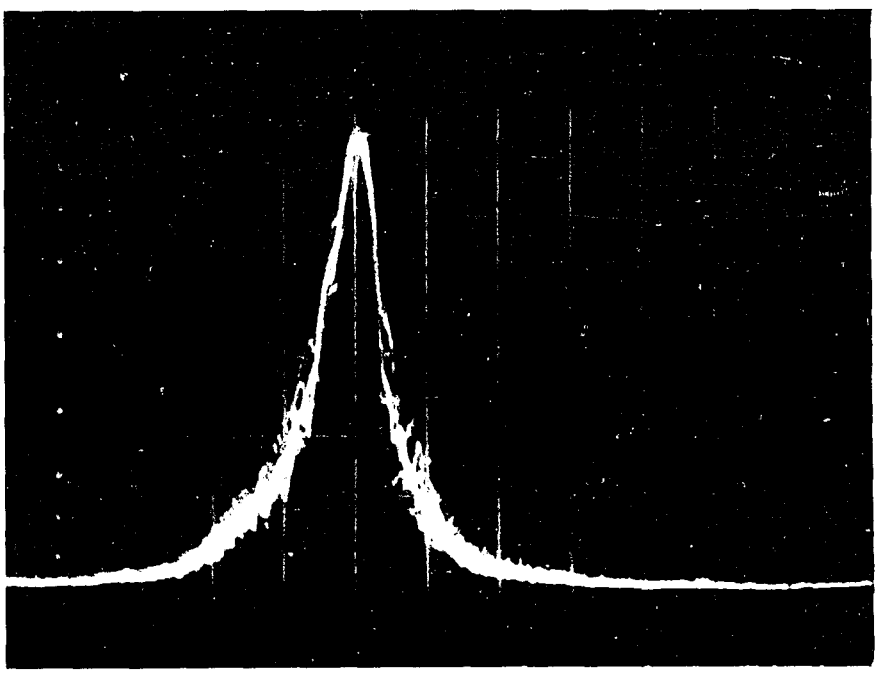

Fig. 10. A Typical Beat Note Spectrum

Vertical Scale: linear

Horizontal Scale: 1 KHz/division

$P_{out} \simeq 15$ μ watts, $\Delta\nu_o \simeq 10$ Hz

Science Building. Best results were usually obtained between 1 and 5 o'clock in the morning.

The width of this spectrum at half maximum is approximately 1.1 KHz. The sweep rate was 60 sweeps per second. Approximately 6 sweeps are visible and the maximum jitter is approximately 1/4 division or 250 Hertz. Assuming that the jitter is caused by disturbances that are not the same for both lasers, we calculate that during times of the order of 100 milliseconds, both lasers experience nearly the same ΔL due to the environment. The differential motion $\Delta \ell$ is

$$\Delta \ell = \frac{\Delta \nu}{\nu} L$$

$$\simeq \frac{250 \times 10}{10^{14}} = 2.5 \times 10^{-11} \text{ cm}$$

Thus, both cavities changed their average lengths by the same amount to the order of 1/200 the size of an atom. This picture demonstrates that the dual laser structure was doing extremely well at minimizing the effects of man-made disturbances. It also demonstrates that to detect the effects of quantum noise over the instrument resolution, the laser linewidth needs to be approximately 1 KHz. For long periods of time, it was usually easy to keep this spectrum on a 10 KHz full width display by slowly changing the center frequency control to compensate for slow drift of the beat note center frequency. The signal would slowly

drift in either direction, sometimes making jumps of two or three divisions. Because of the drift and frequency jitter, attempts to improve the spectrum analyzer resolution by decreasing the sweep rate gave an unstable display.

During all runs the instrument was adjusted to give the best display, and then, with these same instrument settings, the spectrum of a test signal displayed. Any additional width or jitter beyond the test signal spectrum was then attributed to the incoming signal from the lasers. The remaining jitter and slow drift are most likely caused by either slow temperature changes of the quartz block, pressure flutter in the gas cells used to tune the lasers to nearly the same frequency, power supply fluctuations, small Brewster angle window tilts, feedback from the lens, detector or beam splitter, or perhaps some other unknown causes. Attempts to determine which of these causes was predominant always seemed to lead to approximately the same display. Table 1 gives a summary of the effects considered to be important in causing unwanted instabilities and remarks on precautions used to control them.

Signal-to-Noise

In the previous section it was shown that the oscillation linewidth of the test laser must be greater than 1 KHz if it is to be easily observed (Fig. 10). To

show that this is possible, requires consideration of the signal-to-noise ratio.

One of the dual-laser oscillators was always operated far above threshold, so that it had a narrow oscillation linewidth (10 Hz). The power output of the other, the test oscillator, was varied from a small value to full power output in order to vary the oscillation linewidth over a wide range to test the relationship

$$\Delta\nu_o = \frac{\pi h\nu(\Delta\nu_c)^2}{P} \tag{59}$$

For ideal heterodyne detection the signal-to-noise power ratio is given by Forrester (1961)

$$\left.\frac{S}{N}\right|_P = \frac{\eta P}{h\nu\Delta f}$$

Here P is the power received, η the quantum efficiency of the detector, and Δf the limiting electrical bandwidth of the system, in this case, the spectrum analyzer resolution. For easy detection, a signal-to-noise power ratio of approximately 10^4 is desirable. Thus, $\Delta\nu_o$ should be greater than 1 KHz when P (Eq. 59) is the minimum detectable power that gives a signal-to-noise ratio of 10^4.

For ideal heterodyne detection, it is necessary to generate more noise current at the output of detector due to local oscillator shot noise than is present with no

power input. The no input power noise current is related to the D* or NEP of the detector as follows:

$$\langle i_N^2 \rangle^{1/2} = \frac{\eta NEP}{h\nu} e = \frac{\eta}{h\nu} \frac{\sqrt{A\Delta f}}{D^*} e$$

The shot noise generated by the local oscillator is

$$\langle i_{L.o.}^2 \rangle^{1/2} = 2eI_{d.c.}\Delta f$$

$$= 2e\eta e \frac{P_{L.o.}}{h\nu} \Delta f$$

For ideal heterodyne detection

$$\langle i_{L.o.}^2 \rangle^{1/2} \geq \langle i_N^2 \rangle^{1/2}$$

so that

$$P_{L.o.} \geq \frac{\eta}{2h\nu} \frac{A}{D^{*2}} = \frac{\eta}{2h\nu} \frac{(NEP)^2}{\Delta f}$$

For the Philco L4530 detector used;

$$D^* \simeq 10^9 \text{ cm/watt}$$

$$A = 1.33 \times 10^{-4} \text{ cm}^2$$

$$\eta = 1/3$$

Therefore,

$$P_{L.o.} \geq 200\mu \text{ watts}$$

The maximum local oscillator power available from our laser was 15μ watts. Therefore, the ideal

signal-to-noise ratio was reduced by a factor

$$k = \frac{P_{L.o.\ \text{Available}}}{P_{L.o.\ \text{Required}}} = \frac{15 \times 10^{-6}}{200 \times 10^{-6}}$$

$$\simeq 10^{-1}$$

Assuming that the power received by the detector is one-half the laser output power, the effective signal-to-noise ratio, $\frac{S}{N}|_{eff}$, becomes

$$\frac{S}{N}|_{eff} = k \frac{\eta P}{2h\nu\Delta f}$$

Using Eq. (59) and substituting for P,

$$(\Delta\nu_o)(\frac{S}{N})_{eff} = \frac{k\eta\pi(\Delta\nu_c)^2}{2\Delta f}$$

$$= \frac{\pi P_{L.o.}(\Delta\nu_c D^*)^2}{h\nu\Delta f A}$$

For

$$\Delta f = 1 \text{ KHz}$$

$$\Delta\nu_c = 30 \text{ MHz}$$

$$\Delta\nu_o(\frac{S}{N})_{eff} \simeq 10^{10}$$

With a $\frac{S}{N})_{eff} = 10^4$, a $\Delta\nu_o$ of 10^5 should be detectable. This corresponds to a power output of 10^{-10} watts. Thus, a $\Delta\nu_{osc}$ of 10 KHz ($P = 10^{-8}$ watts) should be easily detectable.

We estimate the power output at threshold by using an expression given by Haus (1967).

$$P_{th} = \sqrt{\frac{3}{8}h\nu\omega_o \frac{C}{L}A(t_1+t_2)^2}$$

Here ω_o is the saturation parameter, L the length, A the mode volume, and t_2 and t_1 the mirror transmission factors. Using the following parameters,

$$t_1 + t_2 \simeq .4$$

$$A = \frac{1}{5}(\frac{\pi D^2}{4}) = 3 \times 10^{-3} \text{ cm}^2$$

$$L = 10 \text{ cm}$$

$$\omega_o = 10^{-3} \text{ watts/cm}^2$$

we calculate that

$$P_{th} \simeq 6 \times 10^{-9} \text{ watts}$$

Thus, oscillation linewidths near the threshold region should be observable.

Design Details

The Cavity

Because the 3.39μ laser transition has high gain, the laser cavities of the dual laser structure had to be carefully designed for single longitudinal mode oscillation. The overall cavity length, the bore diameter, and

the mirror reflectivities were chosen for this purpose. The bore diameter was 5 mm because this was the smallest size diamond drill available without special order. A smaller diameter bore would probably have been a better choice because the gain changes in inverse proportion to the bore diameter. A higher gain would have allowed a larger $\Delta\nu_c$ and thus a broader $\Delta\nu_o$. We chose an initial cavity length of 10 cm; however, as the design progressed, a 2.5 cm gas tuning cell was added to the cavity making the overall length 12.5 cm. For this length cavity, the longitudinal modes are spaced by $\Delta\nu_\ell = \frac{C}{2L} \simeq 1200$ MHz. Since the dappler broadened, 3.39μ, He-Ne laser transition is approximately 300 MHz, only one longitudinal mode at a time had significant gain.

In order to eliminate higher order modes, we chose a nearly folded confocal cavity because it has the highest diffraction loss discrimination of any stable cavity. For this cavity the lowest order off axis mode within the atomic linewidth is the $TEM_{\|q-1}$. Because we wanted to keep this mode from oscillating we required that

$$e^{2\alpha_m L} R_1 R_2 R_{d_\|} < 1$$

Here, R_1 = dielectric mirror reflectivity

R_2 = gold mirror reflectivity = .98

$R_{d_{\|}}$ = 1-diffraction losses for the TEM mode

$\alpha_m = 7.2 \times 10^{-2}$ cm^{-1} (5 mm diameter tube)

Therefore,

$$R_1 R_2 R_{d_{\|}} = R_1(.98)R_d < .392$$

or

$$R_1 R_{d_{\|}} < .40 \tag{63}$$

Since the cavity bandwidth is related to the cavity parameters as follows,

$$\Delta\nu_c = -\left(\frac{C}{2L}\right)\left(\frac{1}{2\pi}\right) \ell n(R_1 R_2 R_{d_{oo}}) = 30 \text{ MHz}$$

Then,

$$R_1 R_{d_{oo}} = .90 \tag{64}$$

Here, $R_{d_{oo}}$ = 1-diffraction losses for the TEM_{oo} mode. Taking the ratio of Eq. (64) and Eq. (63) we calculate that

$$\frac{R_{d_{oo}}}{R_{d_{\|}}} \geq \frac{9}{4} = 2.25 \tag{65}$$

When we used this relationship and the results of Fox and Li (1961) relating loss per mirror bounce and cavity Fresnel number for a confocal cavity, we were able to decide upon a cavity Fresnel number N = .65. The losses for this Fresnel number satisfied the constraint of Eq. (65). From the Fresnel number, we calculated the required

mirror diameter, and read the diffraction losses from the theoretical curve. The results are the following:

$$N = \frac{a^2}{(2L)\lambda} = .65$$

$$2a = \text{mirror diameter} = 1.32 \text{ mm}$$

$$R_{d_{oo}} = .98$$

We can then choose the required mirror reflectivity by using Eq. (64). Thus,

$$R_1 = \frac{.90}{R_{d_{oo}}} = \frac{.90}{.98} = .92$$

The initial design of the test oscillator is illustrated in Fig. 11.

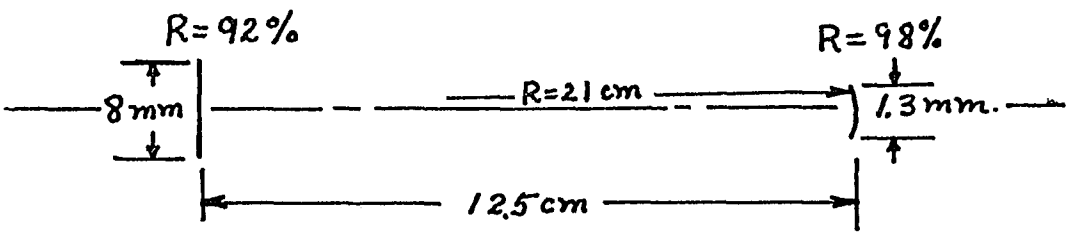

Fig. 11. Test Laser Cavity Dimensions

The local oscillator cavity was designed for maximum single mode output power using the theory of Smith (1966). The reflectivities were found to be sufficiently close to those for the test oscillator so that

the coatings for both oscillators were made at the same time. Thus, Fig. 11 also represents the local oscillator design.

Gas Tuning Cells

The gas cells at the end of the lasers, formed with an optically contacted Brewster angle window to fix the polarization, were used to tune the resonant frequencies of the cavities to near atomic line center, and also to make the beat note be several megahertz for display on the spectrum analyzer. We changed the optical path length of the resonant cavity by pumping the air out of the cell. Using this technique it was easy to slowly tune the cavity resonant frequency over two free-spectral ranges.

Combining Optics

The beam splitter-mirror arrangement was designed in one piece so that independent movement of either of the combining elements (this would cause undesirable frequency flutter in the beat note) was minimized. The barium fluoride beam splitter had a 50-50 dielectric coating on one-half of the front surface and an aluminum coating on the back surface. A quartz lens with approximately a 2 inch focal length, focused the combined beams onto the detector.

The Detector

The indium arsenide detector was ordered with a small area (1.33×10^{-4} cm^2) so that the D* of the detector was large (D* = 6.6×10^9 cm/watt). This was necessary because of the small amount of local oscillator power available. The spectrum analyzer was an SPA-25 Singer Metric panoramic spectrum analyzer used with a Model PRB-1a high impedance probe.

Alignment

The system was aligned in visible light using two Davidson alignment telescopes. First we aligned the telescopes along the optic axis of the laser cavity and then overlapped the two projected images on the detector. A final touch up alignment was made with the lasers running. The criteria for a good alignment was that the detector was in the proper position to obtain maximum response from either laser.

Experimental Difficulties

The major difficulty with the experiment was one of mechanics rather than concept. After the first construction broke, several different attempts were made to attach the gas ballasts to the quartz block. Each of these attempts involved a considerable amount of time because the lasers had to be reassembled, baked out and pumped down, then run continuously on the gas filling station for

approximately one week. After approximately 2-1/2 years a marginal system was finally built using Omni-seal and Emerson Cummings 285 with Catalyst 11. Through all of this work John Poulos of the Optical Science Department was of continual help and encouragement, showing me how to use vacuum equipment, leak detection equipment, high vacuum technique, what good glass blowing looks like, and a variety of other experimental tricks which only he seemed to know. His help was very much appreciated.

If a similar type laser is built again, I would suggest the following:

1. Use "ULE" or "CERVIT" glass instead of quartz. These glasses have lower thermal expansion coefficients, can be optically contacted to other pieces of the same material, and in most other ways are nearly the same as quartz glass.
2. Optically contact or fuse all components to the body of the laser whenever possible. Hardly any epoxy cements will withstand temperatures above 100°C and still have good high vacuum properties. We found the best cements for this type of work to be the following:
   a. Torr-Seal--Good high vacuum properties to about 80°C. Good mechanical strength and an expansion coefficient that will work with quartz glass.

b. Omni-Seal--Good high vacuum properties above 150°C; however, it is runny, has little mechanical strength, and needs to be cured at a high temperature. It can be obtained with a coefficient of expansion that matches quartz glass.

c. Emmerson Cummings 285 with catalyst 11--Good high vacuum properties at temperatures up to approximately 150°C. However, it is brittle, and its coefficient of expansion only marginally matches the expansion coefficient of quartz glass so that a slight tap can crack it away.

CHAPTER IV

DISCUSSION OF EXPERIMENTAL RESULTS

The experimental measurements of the oscillation linewidth using the dual-laser design are presented in Figs. 13 to 19. Figure 12 is a picture of the experimental arrangement. The quantitative results are meager, and there are not enough of them to make definite statements about the correctness or incorrectness of the linewidth expressions derived in Chapter III. However, qualitatively the pictures of the spectrum exhibit with certainty the effects of quantum noise. The noise definitely gets more pronounced, and the spectral width increases with decreasing power and increasing $\Delta\nu_c$. This is in agreement with Eq. (59).

As stated in Chapter III, all of these pictures were taken on an SPA/25 Singer Metric panoramic spectrum analyzer. The dual laser was placed on granite slab that floated on inner tubes in the basement of the Optical Sciences Building. A plywood box and then two other boxes of fiberglass were placed around the equipment on the slab. Both power supplies were run from the same crystal. All the measuring equipment was placed in an adjacent room. The lasers were always run for at least 5 hours before any

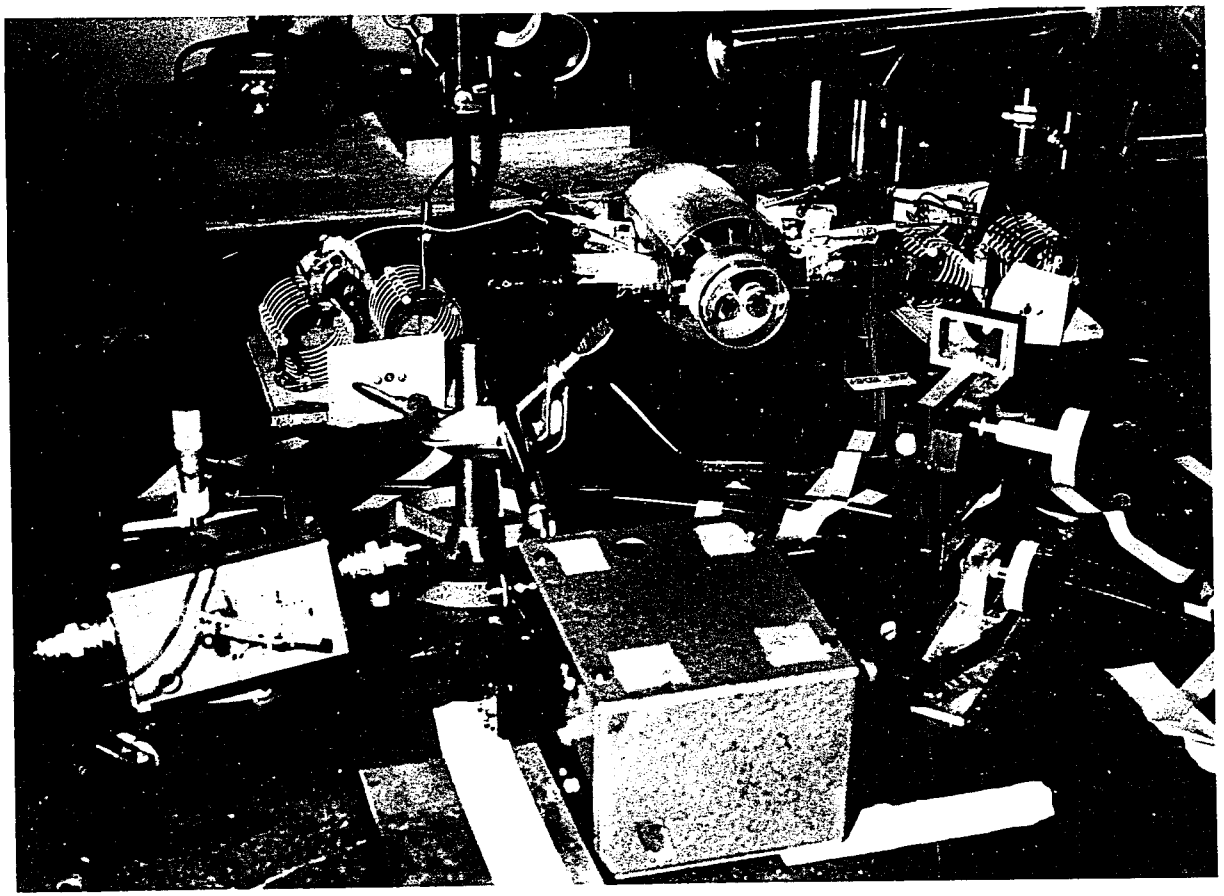

Fig. 12. The Experiment

measurements could be taken because of the slow drift due to heating up of the block from the gas discharge. All the measurements were taken in the dead of night. The beat note was usually quietest between 1 a.m. and 5 a.m. Every time the power level was changed so that the linewidth could be broadened, a few hours were allowed for the temperature of the laser to come to equilibrium. The measurements shown were taken on two different nights.

Typically a picture was taken in the following manner: First, one laser was tuned to near line center by chopping the laser output and observing the chopped signal on an oscilloscope. The center of the atomic line was recognized by tuning the laser through the Lamb dip and then back to near the center of the dip. Then, the second laser was tuned until a zero beat was observed on the oscilloscope. The box was then opened, and the size of the chopped signal measured so that the power of each laser could be determined. The oscilloscope was unplugged and the spectrum analyzer connected. The box was closed and the laser allowed to stabilize. There would be some drift --usually approximately 10 MHz--before the beat would settle down. It was then tuned to a lower frequency--a few megahertz--for observation. When the spectrum looked the quietest (it would sometimes stay at nearly one spot for a few seconds at a time) a picture was taken. If it was a good picture, then without changing the settings on

the spectrum analyzer, a signal from an r-f signal generator was applied, and a picture was taken of the spectrum analyzer resolution for that setting. The resolution was always near to the optimum value for the particular settings used.

The power output of each laser was calculated from the measured voltage in the following way.

$$V = iR_{eq} = \frac{\eta \mathbf{P}}{h\nu} eR_{eq}$$

where η = quantum efficiency = 1/3

e = electronic charge

$\mathbf{P}$ = power at detector $\simeq \frac{P}{2}$

$h\nu$ - energy of 3.39μ quanta

R_{eq} = Equivalent resistance of the detector load resistor and the diode dynamic resistance at the operating point [$R_{eq} = 51^{k}//30^{k} = 19^{k}$]

The cavity bandwidth was calculated using Eq. (56)

$$\Delta\nu_c = -\frac{1}{2\pi}\left(\frac{C}{2L}\right) \ell n R_1 R_2 R_{d_{oo}} \qquad (66)$$

where R_1 = reflectivity of dielectric mirror (measured) = .94

R_2 = reflectivity of gold mirror .98 (handbook)

$R_{d_{oo}}$ = 1-diffraction losses for TEM_{oo} mode

= .98 (calculated)

The measured spectral widths were compared with the oscillation linewidths calculated using

$$\Delta\nu_o = \frac{\pi h\nu(\Delta\nu_c)^2}{P} \tag{67}$$

Figures 13 and 14 were taken with both lasers well above threshold. For these measurements, $\Delta\nu_c$ = 30 MHz, and $\Delta\nu_o \simeq$ 10 Hz, much less than the spectrum analyzer resolution. These pictures are intended to show the stability of the spectrum that was usually observed. Figure 13 shows that there were times when the frequency flutter due to man-made noise was small compared to the width of the spectrum. This picture indicates that for pictures taken at lower powers (Fig. 16) the additional noise is caused by quantum noise. Figure 14 shows a double exposure of the spectrum taken approximately 10 sec apart. The first picture indicates that at times the spectrum was stable for fairly long periods of time. However, the random jumps in the double exposure of the second picture show why the resolution could not be improved; when the resolution was narrowed, the jumps and drift caused the display to be unstable.

Figure 15 should be compared with Fig. 13. The operating conditions were essentially the same, except that the dielectric mirror for one of the lasers was changed from 94% to 72%, thus making $\Delta\nu_c$, and therefore also $\Delta\nu_o$,

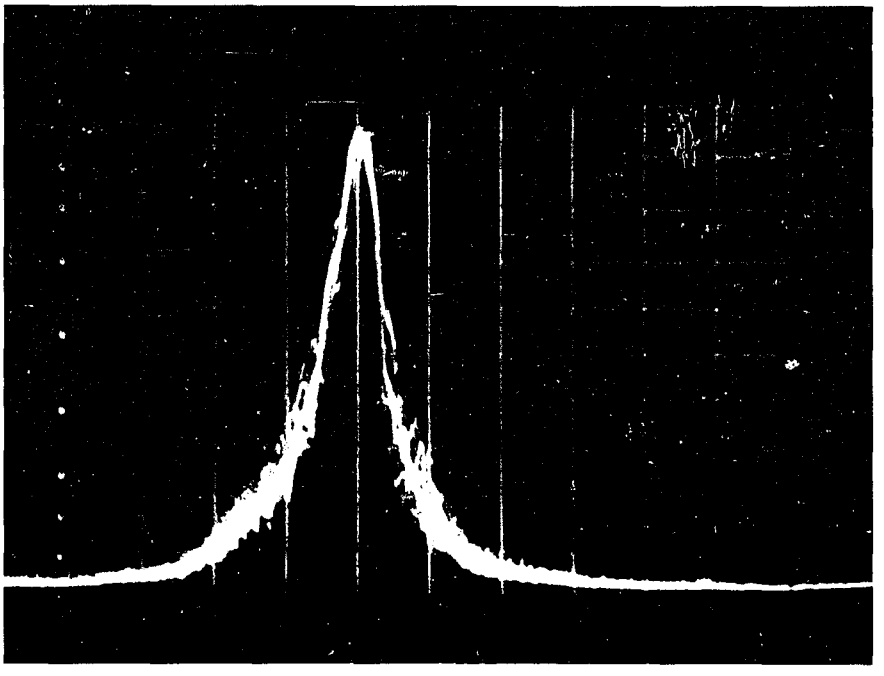

Fig. 13. Typical Beat Note Stability

Dispersion: 1 KHz/division

Power: $P_1 = P_2 \simeq 15$ μ watts

$\Delta\nu_o = 10$ Hz

$\Delta\nu_c = 30$ MHz

Vertical Scale: linear

Horizontal Scale: frequency

Sweep rate: 60 sweeps/sec

Camera setting: f/2 - 1/100 sec

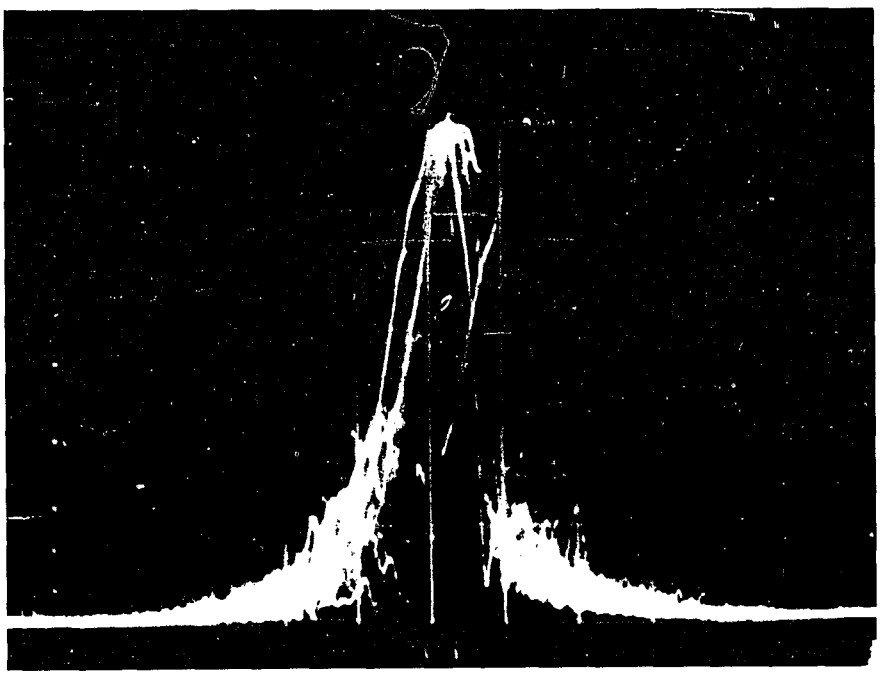

Fig. 14. Long Time Exposure of the Beat Note

Dispersion: 1.5 KHz/division

Power: Both oscillators well above threshold

$\Delta\nu_o$ = 10 Hz

$\Delta\nu_c$ = 30 MHz

Vertical Scale: linear

Horizontal Scale: frequency

Sweep rate: 60 sweeps/sec

Camera setting: f/2 - 1/100 sec

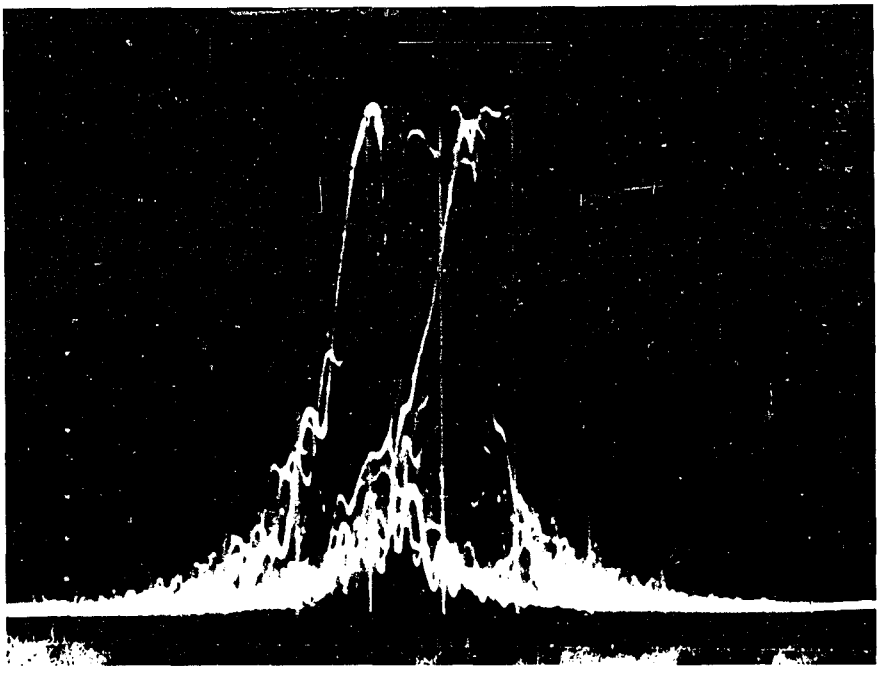

Fig. 14.--Continued

Dispersion: 1.5 KHz/division

Power: Both oscillators well above threshold

$\Delta\nu_o \simeq 10$ Hz

$\Delta\nu_c = 30$ MHz

Vertical Scale: linear

Horizontal Scale: frequency

Sweep rate: 60 sweeps/sec

Camera setting: f/2 - 1/100 sec

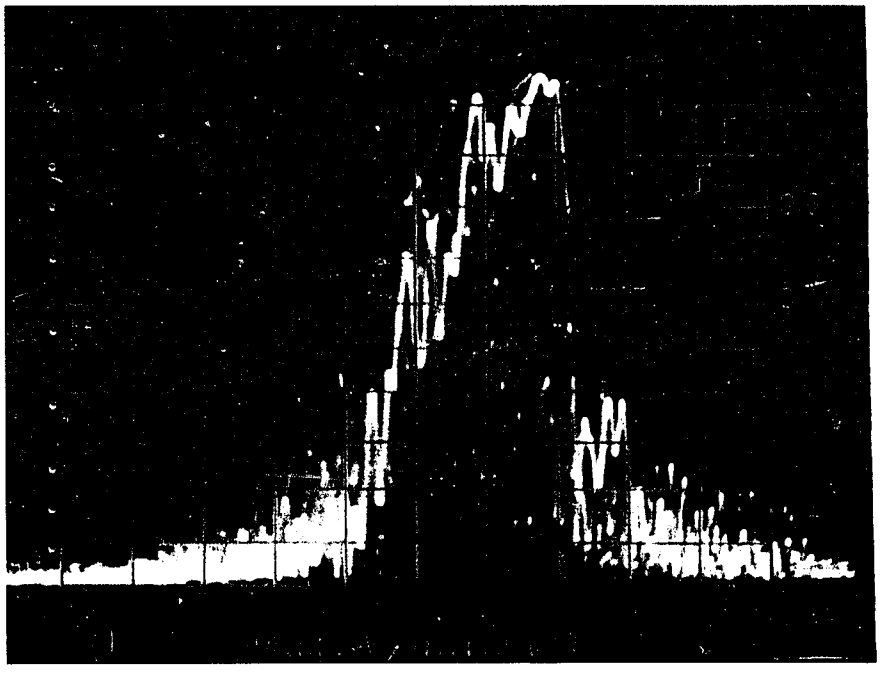

Fig. 15. The Effect of Increasing the Cavity Bandwidth

Dispersion: .9 KHz/division

P_1 = 10 μ watts, $\Delta\nu_o$ = 10 Hz, $\Delta\nu_c$ = 30 MHz

P_2 = 5 μ watts, $\Delta\nu_o$ = 110 Hz, $\Delta\nu_c$ = 61 MHz

Vertical Scale: linear

Horizontal Scale: frequency

Sweep rate: 25 sweeps/sec

Exposure: f/2.8 - 1/50 sec

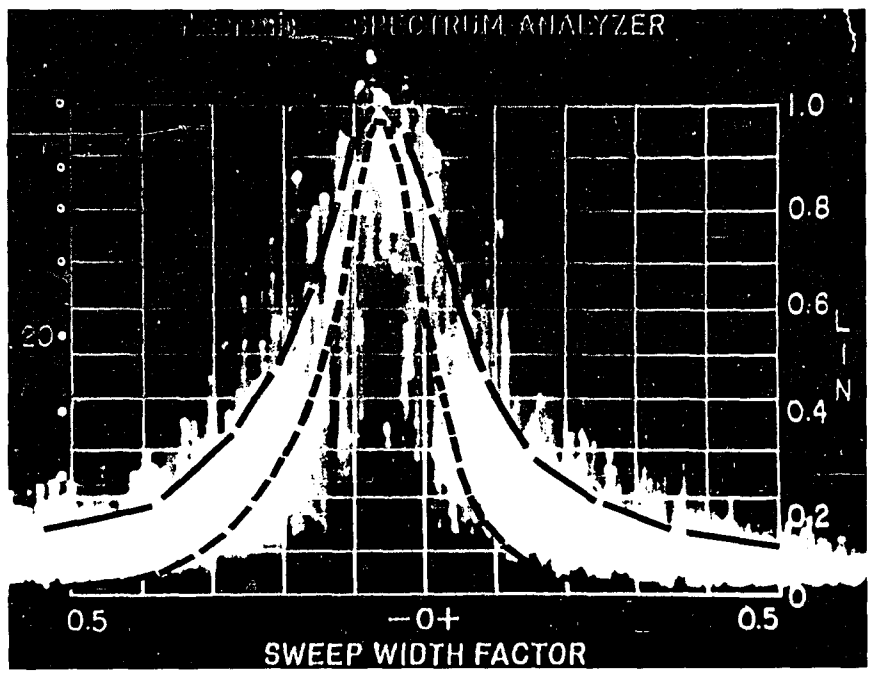

Fig. 16. The Effect of Decreasing the Power

Dispersion: 3.2 KHz/division

P_1 = 10 μ watts, $\Delta\nu_c$ = 30 MHz, $\Delta\nu_o$ = 10 Hz

P_2 = 3 x 10^{-7} watts, $\Delta\nu_c$ = 61 MHz, $\Delta\nu_o$ = 1.8 Hz

Sweep rate: 20 sweeps/sec

Exposure: f/2.8 - 1/50 sec

Curve A: (inner curve) Spectrum Analyzer Resolution

Curve B: (outer curve) Signal Spectrum

larger for the test laser. The additional noise is caused by spontaneous emission--quantum noise.

In Fig. 16 the power was lowered so that the oscillation linewidth of the test laser was approximately equal to the spectrum analyzer resolution. Since the convolution of two Lorentzian spectra is also Lorentzian with a width equal to sum of the two widths (Appendix B), and since the spectrum analyzer displays the convolution of the Lorentzian resolution curve of analyzer with the Lorentzian spectrum of the incoming signal, the plotted spectrum should be wider than the spectrum analyzer resolution--Curve A. Clearly the total spectrum is wider than the resolution curve. There are many curves that could be drawn through the noisy signal spectrum and a quantitative measurement of the oscillation linewidth would be extremely risky. About all that is certain is that the spectrum is broader and noisier than the resolution curve, and that this must be caused by quantum noise. However, this picture is essentially the same type as the laser diode spectrum picture of Hinkley and Freed (1969) (Fig. 2). Their experimental curve was drawn along the outer edge of the noisy spectrum. If we draw a similar curve, Curve B, the spectrum is very nearly Lorentzian with a full width at half-maximum of 8.9 KHz. When we subtract the 4.8 KHz full width at half maximum of the spectrum analyzer resolution we find an oscillation linewidth of 4.1 KHz

compared to the calculated width 1.8 KHz. The measured width is 2.3 times as large as the width calculated by using the simple expression Eq. (67). This extra factor could be attributed to the $\frac{1}{2}(\frac{N_2+N_1}{N_2-N_1})$ term in Eq. (12). In fact Manes (1970) reports that for a similar 3.39μ laser this excess factor is between 1.5 and 2. Using these data then the 4.1 KHz measurement is reasonable.

Figure 17 is similar to Fig. 16 except that the power of the test laser has been lowered to broaden the spectrum. The dotted spectra are the same as before except that the resolution curve is for the new settings. The measured spectral width is 7.7 KHz; the resolution width is 2.2 KHz, leaving a $\Delta\nu_o$ = 5.5 KHz compared to a 5 KHz calculated value. For perfect agreement the excess factor should be 1.1. However, according to Manes (1970) the excess factor should decrease with decreasing power output, so that the smaller excess factor required is still reasonable.

Figures 18 and 19 show the spectrum at a slightly lower power. No estimate of the oscillation linewidth is made because of the uncertainty in the measured power and the noisy signal spectrum.

These pictures represent the best results obtained before one of the lasers ceased to function. I believe that they are sufficient to demonstrate that the quantum

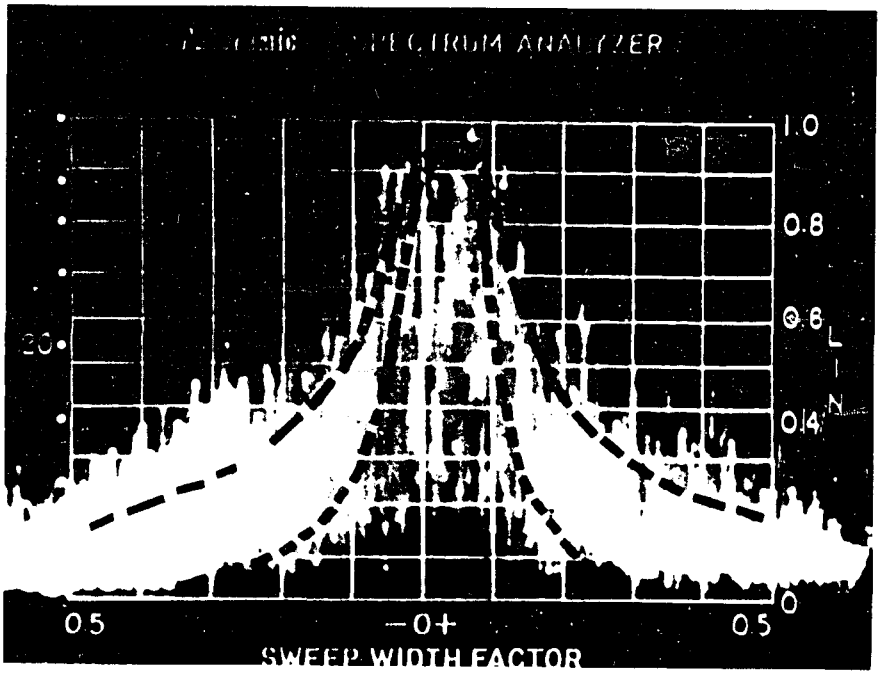

Fig. 17. Laser Linewidth at Low Power

Dispersion: 2.2 KHz/division

P_1 = 10 μ watts, $\Delta\nu_c$ = 30 MHz, $\Delta\nu_o$ = 10 Hz

$P_2 \simeq 10^{-7}$ watts, $\Delta\nu_c$ = 61 MHz, $\Delta\nu_o \simeq$ 5 KHz

Sweep rate: 12 sweeps/sec

Exposure: f/2.8 - 1/50 sec

Curve A: (inner curve) Spectrum Analyzer Resolution

Curve B: (outer curve) Signal Spectrum

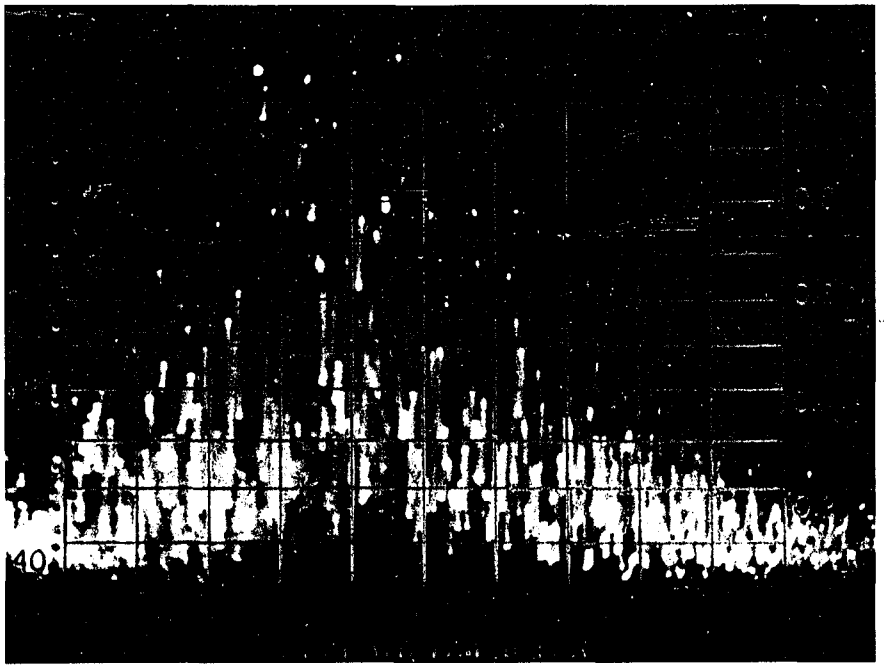

Fig. 18. Laser Linewidth Close to Oscillation Threshold

Dispersion: 2 KHz/division

P_1 = 10 μ watts, $\Delta\nu_c$ = 30 MHz, $\Delta\nu_o$ = 10 Hz

$P_2 \leq 10^{-7}$ watts, $\Delta\nu_c$ = 61 MHz, $\Delta\nu_o$ < 5 KHz

Sweep rate: 25 sweeps/sec

Exposure: f/2.8 - 1/50 sec

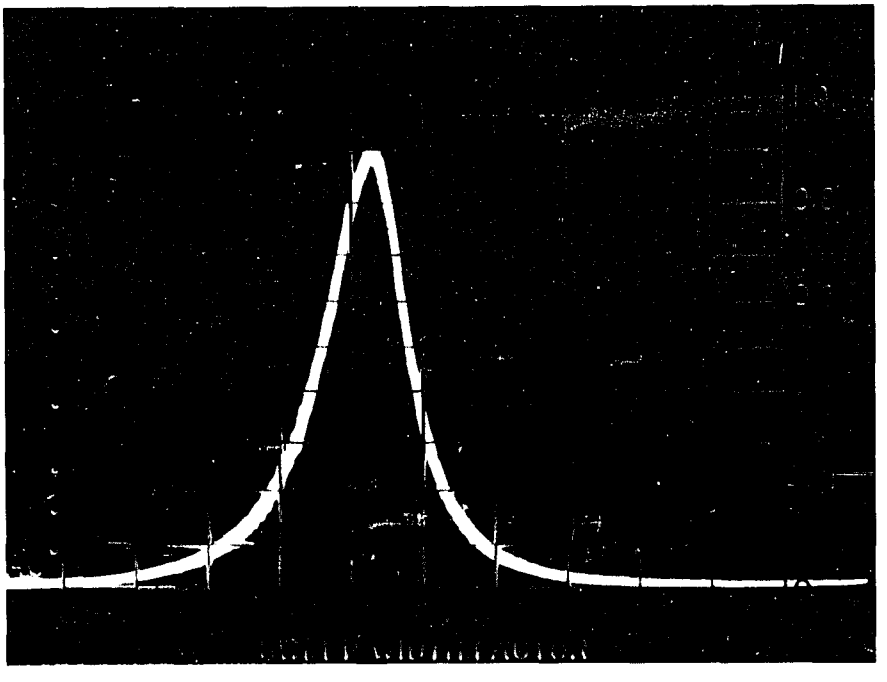

Fig. 19. Spectrum Analyzer Resolution for Fig. 18

noise phase spectrum of a He-Ne 3.39μ laser can be measured using the dual laser design.

More careful measurements that extend the range of observation could be made. However, I feel that the indirect technique used by Manes and Siegman gives better control over the experimental variables and is a better approach. In particular the electronic feedback system that they use (bandwidth approximately 1 Hz) corrects for the slow frequency jitter of the center frequency that caused measurement problems. With such a system better resolution is possible. In fact, using the indirect technique for measuring the laser linewidth as described in Chapter I laser linewidths as small as a few Hz have been measured. Since Manes has recently indirectly measured the oscillation linewidth of the He-Ne 3.39μ lasers it does not seem profitable to continue these measurements.

In conclusion, beat note spectra of two independently operated lasers built into a single quartz block have been measured, the effects of quantum noise observed, relative stability of the dual lasers has been evaluated, and a simple, theoretical derivation of the oscillation linewidth that can be used in a beginning laser course without drawing on artificial analogies has been given.

APPENDIX A

EFFECTS OF AMPLITUDE NOISE

In this appendix, the effects of amplitude noise on the spectrum of laser light is examined. The correlation function for the standing wave field magnitude is written as

$$R_{|E|}(\tau) = \langle |E(t)||E(t+\tau)| \rangle$$

Assuming that the total field amplitude can be written as a steady state field E_o plus a small fluctuating field $e(t)$, $R_{|E|}(\tau)$ can be written as

$$\begin{aligned} R_{|E|}(\tau) &= \langle \left[E_o + e(t)\right] \left[E_o + e(t+\tau)\right] \rangle \\ &= \langle E_o^2 \rangle + E_o[\langle e(t) \rangle + \langle e(t+\tau) \rangle] + \langle e(t)e(t+\tau) \rangle \\ &= E_o^2 + \langle e(t)e(t+\tau) \rangle \end{aligned}$$

This follows from the noise model, Fig. 1, since

$$\langle e(t) \rangle = \langle e(t+\tau) \rangle = 0$$

The fluctuating field $e(t)$ is given by Eq. (57), and written as

$$e(t) = \sum_j \frac{\Delta E_j}{2\beta E_o^2} \delta(t-t_j)$$

where

$$\Delta E_j = \left(\left(\frac{\hbar\omega}{2\epsilon_o V}\right)\right)^{1/2}$$

The analysis for finding the correlation function of e(t) is the same as that leading to Eq. (46), with $\delta\phi_j$ replaced by $\Delta E_{\parallel_j}/2\beta E_o^2$. Therefore, using Eq. (46),

$$\langle e(t)e(t+\tau)\rangle = \mu \frac{\langle(\Delta E_{\parallel_j})^2\rangle}{(2\beta E_o^2)^2}\,\delta(\tau)$$

$$= \frac{\hbar\omega_o \Delta\omega_c}{8\beta^2 E_o^4 \epsilon_o V}\left[(\bar{n} + \frac{1}{2}) + \frac{1}{2}\left(\frac{N_2 + N_1}{N_2 - N_1}\right)\right]$$

and

$$R_{|E|}(\tau) = E_o^2 + \frac{\pi\hbar\omega_o \Delta\omega_c}{8\beta^2 E_o^4 \epsilon_o V}\left[\bar{n} + \frac{1}{2} + \frac{1}{2}\left[\frac{N_2 + N_1}{N_2 - N_1}\right]\right]$$

Taking the Fourier Transform to find the power spectrum,

$$S_{|E|}(f) = E_o^2\delta(f) + \frac{\hbar\omega_o \Delta\omega_c}{8\beta^2 E_o^4 \epsilon_o V}\left[\bar{n} + \frac{1}{2} + \frac{1}{2}\left[\frac{N_2 + N_1}{N_2 - N_1}\right]\right]$$

In order that amplitude noise not effect a phase noise measurement, the second term, the white noise term, must be much smaller than the peak of the Lorentzian phase spectrum, Eq. (4). Therefore,

$$\frac{\hbar\omega_o \Delta\omega_c}{8\beta^2 E_o^4 \epsilon_o V}\left[\bar{n} + \frac{1}{2} + \frac{1}{2}\left(\frac{N_2 + N_1}{N_2 - N_1}\right)\right] << \frac{E_o^2}{\Delta\omega_o}$$

Using Eq. (12), this inequality can be rewritten as

$$\Delta\omega_o << 2\beta E_o^2 = 2(\alpha_t - \ell_t) \sim 10^8 \text{ sec}^{-1}$$

In the region above threshold, $\Delta\omega_{osc}$ is always less than 10^8 radians/sec, so that the amplitude noise spectrum is negligible compared to the phase noise spectrum, and therefore the shape of the r-f spectrum of the total field is due almost entirely to phase noise.

In a heterodyne experiment the spectrum displayed on the spectrum analyzer is proportional to the spectrum of the input signal convolved with the spectrum analyzer resolution spectrum, $S_A(\omega)$. The input signal to the spectrum analyzer is proportional to the diode current which is proportional to the square of the incident field from the two oscillators. Thus,

$$i\alpha[E_{o_1}+e_1(t)]\cos\left|\omega_{o_1}t+\phi_1(t)\right|[E_{o_2}+e_2(t)]\cos\left|\omega_{o_2}t+\phi_2(t)\right|$$

$$= [E_{o_1}E_{o_2}+E_{o_1}e_2(t)+E_{o_2}e_1(t)+e_1(t)e_2(t)]$$

$$\cos\left|\omega_{o_1}t+\phi_1(t)\right|\cos\left|\omega_{o_2}t+\phi_2(t)\right|$$

$$\simeq \frac{E_{o_1}E_{o_2}}{2}\cos[(\omega_{o_2}-\omega_{o_1})t+\phi_2(t)-\phi_1(t)]$$

The analysis giving the spectrum of this signal, $S_i(\omega)$ is the same as that leading to Eq. (1), so that

$$S_i(\omega) = \frac{E_{o_1} E_{o_2}}{2} \int_{-\infty}^{\infty} \left(e^{-i[\omega-(\omega_{o_2}-\omega_{o_1})]\tau} \right.$$

$$\left. e^{-\frac{1}{2}\langle \left| \phi_2(\tau)-\phi_1(\tau)-\phi_2(0)-\phi_1(0) \right|^2 \rangle} \right) d\tau$$

$$= \frac{E_{o_1} E_{o_2}}{2} \int_{-\infty}^{\infty} e^{-i(\omega-\omega_d)\tau} \; e^{-\frac{1}{2}\langle \left| \phi_2(\tau)-\phi_2(0) \right|^2 \rangle}$$

$$e^{-\frac{1}{2}\langle \left| \phi_1(\tau)-\phi_1(0) \right|^2 \rangle} \; d\tau$$

where

$$\omega_d = \omega_{o_2} - \omega_{o_1}$$

and

$$\langle \left| \phi_2(\tau)-\phi_2(0)-\phi_1(\tau)-\phi_1(0) \right|^2 \rangle$$

$$= \langle \left| \phi_2(\tau)-\phi_2(0) \right|^2 \rangle + \langle \left| \phi_1(\tau)-\phi_1(0) \right|^2 \rangle$$

$$- 2 \left| \langle \phi_1(\tau) \rangle - \langle \phi_1(0) \rangle \right| \left| \langle \phi_2(\tau) \rangle - \langle \phi_2(0) \rangle \right|$$

$$= \langle \left| \phi_2(\tau)-\phi_2(0) \right|^2 \rangle - \langle \left| \phi_1(\tau)-\phi_1(0) \right|^2 \rangle$$

because

$$\langle \phi_1(\tau) \rangle = \langle \phi_1(0) \rangle = 0$$

Thus,

$$S_i(\omega-\omega_d) \; \alpha \; S_{\phi_1}(\omega-\omega_d) * S_{\phi_2}(\omega-\omega_d)$$

where $S_{\phi_1}(\omega)$ and $S_{\phi_2}(\omega)$ are the Fourier Transform of the $e^{-1/2\langle|\phi_2(\tau)-\phi_2(0)|^2\rangle}$ and $e^{-1/2\langle|\phi_1(\tau)-\phi_1(0)|^2\rangle}$ respectively. This r-f spectrum displayed at the difference frequency is given by

$$S_{r\cdot f}(\omega) \propto S_i(\omega) * S_A(\omega)$$

$$= S_{\phi_1}(\omega) * S_{\phi_2}(\omega) * S_A(\omega)$$

For the measurements described in Chapter III, one of the oscillators, the local oscillator, had a very narrow spectrum compared to the test oscillator and the spectrum analyzer resolution, and it could be approximated by a delta function. Its main purpose is to translate the spectrum of the test oscillator to the difference frequency. Therefore, the spectrum displayed on the analyzer has the shape of the phase spectrum of the test oscillator convolved with the spectrum analyzer resolution spectrum.

In contrast to a heterodyne experiment with two oscillators, where it is possible to display the phase spectrum, $S_{\phi}(\omega)$, a homodyne experiment can be used to obtain a signal for display of the amplitude spectrum. In a homodyne experiment the detector current

$$i \propto |E_o+E(t)|^2 \cos^2|\omega_o t+\phi(t)|$$

$$= |E_o+e(t)|^2 \left[\frac{1+\cos|2\omega_o t+2\phi(t)|}{2}\right]$$

Since the photodiode cannot respond to light frequencies, $2\omega_o$,

$$i \alpha \frac{\left|E_o+e(t)\right|^2}{2}$$

The spectrum of this signal is proportional to Fourier transform of the correlation function, $R_e(\tau)$, that is, proportional to the spectrum of the amplitude noise.

APPENDIX B

THE CONVOLUTION OF TWO LORENTZIAN SPECTRA

The spectrum of the convolution of two Lorentzian spectra is also Lorentzian with a width equal to the sum of the Lorentzian linewidths. This can be seen as follows:

Let $S_1(\omega)$ and $S_2(\omega)$ denote the two Lorentzian spectra centered at ω_1 and ω_2, and let S_T denote their convolution. Then

$$S_T(\omega) = S_1(\omega) * S_2(\omega)$$

$$= F_1T_1\left\{\left(e^{-\frac{D_1}{2}|\tau|}\cos\omega_1\tau\right)\left(e^{-\frac{D_2}{2}|\tau|}\cos\omega_2\tau\right)\right\}$$

$$= F_1T_1\left\{e^{-(\frac{D_1+D_2}{2})|\tau|}\cos\omega_1\tau\cos\omega_2\tau\right\}$$

$$= F_1T_1\left\{e^{-\frac{D_1+D_2}{2}|\tau|}\frac{\cos(\omega_2-\omega_1)\tau}{2}\right\}$$

Here $F_1T_1\{\cdot\}$ denotes a Fourier transform. The high frequency term at $\omega_2 + \omega_1$ has been neglected. The result is a Lorentzian spectrum of width $(\frac{D_1+D_2}{2})$, centered at $\omega_2-\omega_1$.

REFERENCES

Arecchi, F. T., V. Degiorgio, and B. Querzola, Phys. Rev. Letters, 1967, 19:1168.

Armstrong, J. A., and A. W. Smith, Phys. Rev. Letters, 1965, 14:68.

Bell, W., and D. Sinclair, Gas Laser Technology, Holt, Rinehart and Winston, 1969.

Feynman, R. P., and A. R. Hibbs, Path Integrals and Quantum Mechanics, McGraw-Hill, 1965.

Forrester, A. T., J. Opt. Soc. Am., 1961, 51:253.

Fox, A. G., and T. Li, Bell System Technical Journal, 1961, 40:453.

Haus, H. A., MIT Internal Memorandum #186, 1967.

Hinkley, E. D., and C. Freed, Phys. Rev. Letters, 1969, 23:277.

Javan, A., E. A. Ballik, and W. L. Bond, J. Opt. Soc. Am., 1962, 52:96.

Lamb, W. E., Phys. Rev., 1964, A134:1429.

Manes, K. R., Ph.D. Thesis, Dept. of Electrical Engineering, Standford University, 1970.

Reif, F., Statistical and Thermal Physics, McGraw-Hill, 1965.

Scully, M., and W. E. Lamb, Phys. Rev. Letters, 1966, 16: 853-855.

Siegman, A. E., B. Diano, and K. R. Manes, IEEE J. Quantum Electronics, 1967, QE-3:180-189.

Smith, P. W., IEEE J. Quantum Electronics, 1966, QE-2:62.